

On Computation of Conditional Mean Spectrum in Eastern Canada

Poulad Daneshvar¹, Najib Bouaanani² and Audrey Godia³

ABSTRACT: This paper investigates the main ingredients required to compute Conditional Mean Spectra (CMS) in Eastern Canada, and assesses their effects on the obtained CMS. We particularly address the influence of ground motion prediction equations (GMPEs) and correlations between spectral accelerations. CMS are computed using two approximate methods and the results are illustrated for three locations with different seismic hazard and risk levels. It is found that selection of GMPEs considerably influences the CMS, particularly at shorter periods. A database of historical records from Eastern Canada is studied to obtain correlation coefficients. The results suggest higher spectral correlations than predicted by a model based on ground motions from Western North America (WNA). The sensitivity of correlation coefficients to magnitude and epicentral distance is also verified, revealing that magnitude has a more significant effect on these coefficients than distance. We also show that the effect of magnitude- or distance-based correlation coefficients on the CMS is: (i) generally negligible at long periods, and (ii) significant at shorter periods particularly when the conditioning period is less than approximately 0.5 s. This work is the first study addressing in detail the ingredients and construction of CMS in Eastern Canada. The methodology and results discussed are expected to enhance the application of CMS in this region.

KEYWORDS: Earthquakes, Conditional mean spectra, Eastern Canada, Ground motion prediction equations, Epsilon, Correlation coefficients for spectral accelerations.

¹ Ph.D. Candidate, Department of Civil, Geological and Mining Engineering, Polytechnique Montréal, Montréal, QC H3C 3A7, Canada

² Professor, Department of Civil, Geological and Mining Engineering, Polytechnique Montréal, Montréal, QC H3C 3A7, Canada. Corresponding author. E-mail: najib.bouaanani@polymtl.ca

³ Research Assistant, Department of Civil, Geological and Mining Engineering, Polytechnique Montréal, Montréal, QC H3C 3A7, Canada

1 Introduction

Dynamic time-history analysis has become a popular method to determine structural response to ground motions. For this purpose, ground motion records are commonly selected and often scaled to match a Uniform Hazard Spectrum (UHS) with a given probability of exceedance (or non exceedance), e.g. 2% in 50 years. The spectral amplitudes provided by the UHS at all considered periods, are those associated with the defined probability of (non)exceedance, and therefore the UHS does not represent each individual spectrum. For this reason and the inherent conservatism associated with the UHS, the appropriateness of using this spectrum as a target for ground motion selection has been criticized. As an alternative, the Conditional Mean Spectrum (CMS) was proposed (Baker and Cornell 2006, Baker 2011). A CMS is a mean response spectrum computed based on the condition that the spectral acceleration matches a target amplitude at a given period. The difference between the target spectral acceleration and that predicted by a ground motion prediction equation (GMPE) at the same period is evaluated as a number of standard deviations associated with this GMPE. This difference, denoted by ϵ , plays a significant role in the construction of CMS. Determination of ϵ values has been widely addressed in the literature (McGuire 1995; Harmsen 2001; Baker and Cornell 2005; Baker and Jayaram 2008; Burks and Baker 2012). Harmsen (2001) provided contour maps of modal and mean ϵ values for Central and Eastern United States (CEUS) and Western United States (WUS) based on probabilistic seismic hazard analysis (PSHA). Burks and Baker (2012) investigated the occurrence of negative ϵ values at short periods particularly in Eastern North America (ENA). The correlation between ϵ values at different periods shapes the CMS in the period range of interest. A number of prediction equations have been proposed to determine the inter-period correlation coefficients based on the period on which the CMS is conditioned (Inoue and Cornell 1990; Baker and Cornell 2006; Baker and Jayaram 2008). The concept of CMS is also gaining attention in ENA which is a region with low to moderate seismic activity. However, the majority of the studies concerning ϵ and CMS have been conducted considering the seismicity of Western North America (WNA). USGS (<http://earthquake.usgs.gov/hazards/apps>, last accessed July 2014) provides PSHA-based CMS and ϵ for both eastern and western regions of the United States. These results are however based on ground motion models adopted to define seismic hazard in the United States. In the absence of correlation models specific to ENA, and Eastern Canada in particular, those developed for regions with higher seismic activity such as WNA have been used instead (Daneshvar et al. 2014). However, the applicability of such models to ENA and mainly Eastern Canada has not been fully addressed.

This work focuses on the ingredients required to construct CMS in Eastern Canada, and investigates the effects of their variations on the constructed CMS. The paper is organized as follows. First, a review of the general steps to construct the CMS is presented in Section 2. In Section 3, we investigate the sensitivity of CMS and ϵ to six different GMPEs including a newly proposed GMPE that accounts for up-to-date seismological characteristics of ENA. In Section 4, correlation coefficients for spectral accelerations specific to Eastern Canada are determined based on historical records, compared to a commonly used WNA correlation model and then their effects on the CMS evaluated. This section also demonstrates the effects of magnitude and epicentral distance on correlation coefficients for Eastern

Canada and the resulting CMS. The findings are illustrated for three locations with low and moderate seismic hazard and risk, i.e. Toronto, Montreal and Quebec.

2 Review of the General Steps to Construct CMS

A general step by step procedure for CMS computation was proposed by Baker (2011). To facilitate appraisal of the different steps of this procedure and its programming, we propose the flowchart illustrated in Fig. 1. The procedure starts with the determination of a target spectral acceleration S_a at the desired period T^* . Provided that the target spectral amplitude is obtained from a probabilistic seismic hazard analysis (PSHA), the mean (or modal) values of magnitude M , epicentral distance R and epsilon $\epsilon(T^*)$ can be taken from the corresponding seismic hazard deaggregation. ϵ is defined as the difference, measured as the number of standard deviations, between the predicted and the target spectral accelerations associated with a specific magnitude M , distance R and period T . Next, a GMPE has to be selected. In the case where a PSHA is used, the same GMPE that produced the mean (modal) values in the previous step can generally be adopted. The spectral predictions of the GMPE are determined for the selected magnitude M and distance R combination in the desired period range. The reported sigma values for the GMPEs at each period are also considered. If a PSHA is not available or the ϵ value is not provided in the deaggregation results, the ϵ value at T^* can be calculated for a specific magnitude M , distance R , and spectral acceleration S_a at this period as (Baker 2011)

$$\epsilon(T^*) = \frac{\ln S_a(T^*) - \mu_{\ln S_a}(M, R, T^*)}{\sigma_{\ln S_a}(T^*)} \quad (1)$$

where $S_a(T^*)$ is the spectral amplitude from the target spectrum, $\mu_{\ln S_a}(M, R, T)$ represents the predictions of the GMPE, and $\sigma_{\ln S_a}(T^*)$ is the standard deviation in logarithmic units provided by the GMPE. Suitable correlation coefficients $\rho(T, T^*)$, such as the ones suggested by Baker and Jayaram (2008), referred to as BJ08 hereafter, are then used to calculate the value of ϵ at other periods T as $\epsilon(T) = \rho(T, T^*) \epsilon(T^*)$. We note that determination of correlation coefficients for Eastern Canada and also applicability of BJ08 to this region is discussed later in Section 4. The CMS $\mu_{\ln S_a(T)}^{(\text{CMS})}$ and the associated conditional standard deviation $\sigma_{\ln S_a(T)}^{(\text{CMS})}$ are obtained as

$$\mu_{\ln S_a(T)}^{(\text{CMS})} = \mu_{\ln S_a}(M, R, T) + \epsilon(T) \sigma_{\ln S_a}(T) = \mu_{\ln S_a}(M, R, T) + \rho(T, T^*) \epsilon(T^*) \sigma_{\ln S_a}(T) \quad (2)$$

and

$$\sigma_{\ln S_a(T)}^{(\text{CMS})} = \sigma_{\ln S_a}(T) \sqrt{1 - \rho^2(T, T^*)} \quad (3)$$

Lin et al. (2013) discussed four approaches, three approximate and one exact, to determine CMS. The proposed methods vary based on the number of considered GMPEs, their corresponding weights in a PSHA-related logic tree and deaggregation, as well as multiple earthquake scenarios contributing to seismic hazard. “Method 1” uses the mean values of the required parameters, e.g. M and R combinations, from deaggregation, and substitutes them into a single GMPE. Eq. (2) is then used to compute CMS. “Method 2”, a refined version of “Method 1”, considers all the GMPEs used to conduct PSHA

and their logic tree weights. The same procedure as “Method 1” is used to compute CMS for each GMPE. The final CMS is obtained by summing up the computed CMS considering their logic tree weights. “Method 3” considers GMPE deaggregations, if available, to determine the mean value of the required parameters to be used with each individual GMPE, e.g. M and R combinations, and next, similar to “Method 1”, the CMS corresponding to each GMPE is computed. “Method 3” also takes, from GMPE deaggregation, the probability that each GMPE predicted exceedance (or occurrence) of $S_a(T)$. The final CMS is computed as the sum of the obtained CMS considering the mentioned probabilities. “Method 4”, the exact method, follows the steps of “Method 3” with the difference that the individual CMS is computed for each set of parameters, e.g. M and R combinations, obtained from PSHA deaggregation results and not only for the mean values of such parameters. The contribution of each of such parameter combinations to exceedance (or occurrence) of $S_a(T)$ is considered in computation of the final CMS similar to “Method 3”. The reader is referred to Lin et al. (2013) for a detailed explanation of the considered parameters and approaches and to Daneshvar et al. (2014) for a step by step construction of CMS to analyze an eight-storey building in Montreal.

3 Construction of CMS for Eastern Canada

Fig. 1 and Section 2 clearly confirm that GMPEs are one of the fundamental ingredients needed to calculate CMS. The effect of varying GMPEs on the resulting CMS and ϵ values is studied in Section 3.2. Such a study requires adoption of “Method 1” in Lin et al. (2013). This method is indeed the only of the four proposed by Lin et al. (2013) that considers a single GMPE which is not necessarily the one used for PSHA or construction of the target UHS. Accordingly, a comparison of the effects of different GMPEs on the resulting CMS considering the same UHS can be carried out. Section 3.1 introduces the GMPEs used in this study.

3.1 Ground Motion Prediction Equations

A variety of GMPEs have been proposed in the literature to predict spectral amplitudes in ENA. The main parameters of some of the GMPEs selected for this study are summarized in Table 1 and are briefly described next.

Silva et al. (2002) proposed a GMPE with different coefficients accounting for single and double corner frequency models with constant and variable stress drops and magnitude saturation. The single corner frequency model with variable stress drop, referred to as SGD02S hereafter, and the double corner frequency model with magnitude saturation, referred to as SGD02D hereafter, are selected for this study. Regression analyses were performed on the data from 13500 simulations. The proposed GMPE covers a Joyner-Boore distance of $1 \leq R_{jb} \leq 400$ km and a moment magnitude (M_W) range of $M_W = 4.5$ to $M_W = 8.5$ for CEUS and ENA hard rock sites.

Atkinson and Boore (2006) developed a set of relationships, referred to as AB06 hereafter, to predict ENA ground motions using a stochastic finite fault model (Hanks and McGuire 1981, Boore 1983). A

data set of 38400 simulated ground motions having magnitudes between $M_W = 3.5$ and $M_W = 8$ and fault distances ranging from 1 km to 1000 km was compiled. Equations to predict the median amplitudes of 5%-damped pseudo-spectral accelerations (PSA) for ENA ground motions were developed through regression analyses of the simulated records. Modifications due to new seismographic data were made to AB06 equations as provided in Atkinson and Boore (2011). The modified version of AB06 is used in this study.

To predict ENA ground motions, Atkinson (2008) adopted a *referenced empirical* approach which combines available data from ENA to that from an active tectonic and better-instrumented reference region, in this case WNA. Based on the same database of ground motions used by Atkinson and Boore (2006), Atkinson (2008) proposed a GMPE, referred to as A08 hereafter, corresponding to ground motion characteristics in ENA while having an overall magnitude scaling behavior of observations in WNA (Atkinson 2008). The database included ENA records with a magnitude range of $M_W = 4.3$ to $M_W = 7.6$. The reference WNA GMPE used is the Boore and Atkinson (2008) relations, modified later by Atkinson and Boore (2011) based on new seismographic data. The Boore and Atkinson (2008) relationships are one of the five sets of equations developed under the Next Generation Attenuation Relationships for Western US (NGA West) program coordinated by Pacific Earthquake Engineering Research Center (PEER). These relationships were based on results from regression analyses on records from shallow crustal ground motions in active tectonic regions compiled in the PEER-NGA West dataset. The equations were developed for a magnitude range of $M_W = 5.0$ to $M_W = 8.0$, closest horizontal distance to the surface projection of the fault plane (R_{jb}) of up to 200 km and a time-averaged shear-wave velocity in the top 30 m (V_{S30}) of $180 \leq V_{S30} \leq 1300$ m/s. The A08 GMPE covers a Joyner-Boore distance range of $1 \leq R_{jb} \leq 1000$ km. It is worth mentioning that the main difference between this referenced empirical approach and the hybrid empirical method proposed by Campbell (2003) is that it directly employs observational ENA ground motion data instead of using a stochastic model. The modified version of A08 (Atkinson and Boore 2011) is used in this study.

Pezeshk et al. (2011) proposed a new GMPE for ENA, referred to as PZT11 hereafter, based on a hybrid empirical method adopting five WNA GMPEs provided by PEER. The GMPEs were developed by Abrahamson and Silva (2008), Boore and Atkinson (2008), Campbell and Bozorgnia (2008), Chiou and Youngs (2008) and Idriss (2008). The new GMPE covers a magnitude range of $M_W = 5$ to $M_W = 8$ and closest distances to the fault rupture (R_{RUP}) of $1 \leq R_{RUP} \leq 1000$ km and is used to generate median 5%-damped pseudo-accelerations in ENA for given magnitude and distance considering hard rock sites, i.e. $V_{S30} \geq 2000$ m/s.

The above-mentioned GMPEs use different distance measures to predict ground motions. To compare the predictions on a uniform distance basis, the equations suggested by Atkinson and Adams (2013) were adopted to convert all distance measures to hypocentral distance, which is the measure used by the Geological Survey of Canada (GSC) for deaggregation results.

3.2 Sensitivity of CMS-shape and ϵ to GMPEs

“Method 1” was introduced by Lin et al. (2013) as one of the approximate methods to compute CMS. It assumes that the target spectrum can be used with a GMPE other than its original underlying GMPE(s). The “Method 1” procedure is similar to that illustrated in Fig. 1. Hence, the UHS prescribed by the National Building Code of Canada (NBCC 2010) considering a return period of 2% in 50 years for three major Eastern Canadian cities: Toronto, Montreal and Quebec, are used as the target spectra in this section. For each location, the underlying deaggregation results provided by GSC, upon request, are consulted to extract the M and R combination corresponding to $S_a(T^*)$ taken from the UHS. These M and R sets are presented in Table 2. Considering structures with fundamental periods of $T^* = 0.2$ s, $T^* = 0.5$ s, $T^* = 1$ s, and $T^* = 2$ s, Eqs. (1), (2) and (3) are used to obtain $\epsilon(T^*)$, $\epsilon(T)$, and the CMS corresponding to each GMPE and T^* . It is noted that the GSC deaggregation is provided for NBCC 2010 site class C and thus the GMPE predictions are modified using the coefficients given in Atkinson and Boore (2011) to correspond to this site class. Furthermore, deaggregation results provided by GSC do not include mean $\epsilon(T)$ values and thus, as mentioned in Section 2, Eq. (1) is used to obtain $\epsilon(T^*)$ and $\epsilon(T)$. Figs. 2 to 4 illustrate the CMS computed using each of the adopted GMPEs and UHS. The level of conservatism included in the UHS in comparison to CMS, as mentioned in Section 1, is clearly observed. We can see that in the cases where the CMS is anchored to the UHS at a short period, i.e. $T^* = 0.2$ s, the accelerations corresponding to the resulting CMS can exceed those of the UHS depending on which GMPE is used. Such an observation is expected as the NBCC 2010 UHS are capped at $T = 0.2$ s, i.e. the spectral accelerations at periods shorter than $T^* = 0.2$ s are equal to that at $T^* = 0.2$ s whereas originally the UHS has a peak at the period range shorter than $T = 0.2$ s. Figs. 2 to 4 also show the variation in CMS amplitudes as a result of changes in the underlying GMPE. The dispersion of CMS amplitudes is more dramatic at the shorter period range where there is larger difference between the predictions of the GMPEs. The broadness of this range depends on the selected T^* . We note that the amplifications observed in the CMS corresponding to Silva et al. (2002) at shorter periods root from the particular spectral shape predicted by SGD02 combined with the correlation coefficients. The epsilon values reported in Figs. 2 to 4 shed more light on the reason behind the variation in CMS amplitudes. It is shown in Eqs. (1) and (2), that the standard deviation and consequently the epsilon corresponding to each GMPE greatly affect CMS amplitudes. The difference between CMS amplitudes and those from the UHS at longer periods partly depends on how far the GMPE predictions are from the UHS. As can be seen in Figs. 2 to 4, the CMS computed using SGD02S can result in overconservative amplitudes when anchored to the UHS at longer periods. This is mainly due to the fact that SGD02S produces conservative spectral amplitudes in comparison to the other GMPEs studied (Atkinson and Adams 2013). As the correlation coefficients for all the illustrated CMS are calculated using BJ08, the only influential factors are the predicted spectral amplitudes and the $\epsilon(T^*)$. The presented results reiterate the approximative nature of “Method 1” and confirm that a certain bias can be introduced when GMPEs other than the one(s) underlying a given UHS are used to generate the CMS. This emphasizes the importance of appropriately selecting GMPEs to construct CMS, especially for structures with relatively short fundamental periods and also those for which higher mode effects are significant.

3.3 Consideration of Multiple GMPEs

Lin et al. (2013) suggest “Method 2” as another approximate approach to compute CMS. “Method 2” is a refined version of “Method 1” in the sense that all the GMPEs used in the PSHA are considered and their corresponding weights in the PSHA logic tree are accounted for. Following Eqs. (4) and (5) are suggested to obtain the CMS and the conditional standard deviations

$$\mu_{\ln S_a(T)}^{(\text{CMS})} = \sum_i P_i \mu_{\ln S_a(T), i}^{(\text{CMS})} \quad (4)$$

and

$$\sigma_{\ln S_a(T)}^{(\text{CMS})} = \sqrt{\sum_i P_i \left\{ \left[\sigma_{\ln S_a(T), i}^{(\text{CMS})} \right]^2 + \left[\mu_{\ln S_a(T), i}^{(\text{CMS})} - \mu_{\ln S_a(T)}^{(\text{CMS})} \right]^2 \right\}} \quad (5)$$

where i is the number of GMPEs and P_i is the weight assigned to the i th GMPE in the PSHA logic tree. To investigate the application of “Method 2” to generate CMS in Eastern Canada, the prescribed NBCC 2010 UHS with 2% in 50 years return period for Toronto, Montreal and Quebec are selected as the target spectra and the ENA GMPE model proposed by Atkinson and Adams (2013) is used to construct CMS. This GMPE, referred to as AA13 hereafter, consists of a representative or central GMPE and upper and lower GMPEs to account for epistemic uncertainty about the central one. The central GMPE is determined by calculating the geometric mean of five peer reviewed GMPEs. The geometric mean \pm its standard deviation is considered as the upper/lower GMPE. The five GMPEs are SGD02S, SGD02D, AB06, A08 and PZT11. The final predictions are provided in terms of moment magnitudes and epicentral distances for B/C, i.e. $V_{s30} = 760$ m/s site condition. The reader is referred to Atkinson and Adams (2013) for more details about the determination of the central, upper and lower GMPEs, the distance metric conversions, and also the conversion factors used to modify the predictions corresponding to different site conditions to represent those of B/C site condition. The CMS computed using the AA13 central GMPE is also included in Figs. 2 to 4 for comparison purposes. The weights assigned to the central, upper and lower GMPEs in PSHA are period-based and are given, respectively, as follows: 0.5, 0.25 and 0.25 for $T \geq 1$ s; 0.4, 0.4 and 0.2 for $T \leq 0.2$ s; and a transition of weights is considered between $T > 0.2$ s and $T < 1.0$ s, e.g. 0.4, 0.35 and 0.25 for $T = 0.5$ s (Atkinson and Adams 2013). The spectral amplitudes corresponding to B/C, i.e. $V_{s30} = 760$ m/s site condition are not provided by GSC for the NBCC 2010 UHS while the GMPEs provide spectral accelerations for B/C site condition. Thus, in order to maintain consistency, period-dependent factors (Atkinson and Boore 2011) are applied to the predictions of the GMPEs to represent NBCC 2010 site class C. The three GMPEs and their corresponding weights are used along with Eqs. (4) and (5) to compute the CMS using “Method 2”. Figs. 5 to 7 show the obtained CMS conditioned on spectral accelerations at $T^* = 0.2$ s, $T^* = 0.5$ s, $T^* = 1$ s, and $T^* = 2$ s. Figs. 5 to 7 also compare the CMS computed using “Method 2” to those computed considering “Method 1” using the AA13 central GMPE and the upper and lower GMPEs, individually. It can be seen that the CMS computed considering the central GMPE using “Method 1” and “Method 2” are very similar. In fact, this similarity is expected as both methods are supposed to produce approximate spectral amplitudes for a particular exact CMS. Slight differences between the CMS obtained from the two methods are observed for short periods. This

roots from the weighting scheme of AA13 at this period range. In general, as the outcome of the two methods are fairly similar, “Method 1”, due to its simplicity, is suggested to be used with AA13 central GMPEs to compute CMS for Eastern Canada. Nevertheless, for structures with very short fundamental periods, using “Method 2” results in more refined CMS as the logic tree weights are also considered in the computations. Indeed, relatively larger differences, through the entire period range considered, could be observed if the upper and lower GMPEs are replaced with those that are not related to the central GMPE. However, the UHS prescribed by NBCC 2010 for Eastern Canada are determined based on the same approach adopted in this study, i.e. central, upper and lower GMPEs.

4 Correlation Model for Spectral Accelerations

4.1 Correlation Coefficients in Eastern Canada

The CMS calculated and presented in Section 3 require the application of a correlation model, as pointed out in Section 2. One of the most commonly used correlation models is the one proposed by Baker and Jayaram (2008) which is developed using four different NGA West GMPEs and considering shallow crustal ground motion records from NGA West ground motion library (<http://peer.berkeley.edu/nga>, last accessed July 2014). The applicability of BJ08 to regions other than WNA was confirmed by Jayaram et al. (2011) who studied Japanese records from a subduction zone and concluded that the BJ08 model, which was developed using shallow crustal earthquakes, can represent the correlations in this region up to an acceptable extent. Lin et al. (2013), although pointing out the lack of data to confirm or reject the applicability of BJ08 model to stable continental sources, conclude that ground motion prediction equations, earthquake magnitude, distance and rupture mechanisms have almost insignificant effects on the correlation models. Lin et al. (2013) also report that the online tool provided by USGS to construct CMS for locations within the United States uses BJ08 model for the Eastern part which is a stable continental seismic zone that can be assumed similar to Eastern Canada. Based on the above discussion, we decided to use BJ08 model to construct the CMS for Toronto, Montreal and Quebec in Section 3.

To the authors’ knowledge, there is no available study on correlation coefficients specific to Eastern Canada and their agreement with the proposed BJ08 model. A major obstacle against the full assessment of ϵ values and the derivation of prediction equations for correlation coefficients in Eastern Canada is the very limited number of records of interest for the engineering community in terms of magnitude and distance. For this reason, model BJ08, developed using WNA records, has been commonly used in the absence of ENA-specific correlation models. The applicability of this model is investigated further herein by comparing its predictions to available observations from Eastern Canada. For this purpose, we compiled a database of 108 horizontal accelerograms from 8 earthquakes with magnitudes M_W from 4.5 to 6.9 and epicentral distances R from 6.8 km to 640 km. All selected ground motions were recorded on hard rock sites, i.e. NBCC 2010 site class A: $V_{S30} \geq 1500$ m/s. A list of the corresponding earthquake events is provided in Table 3. The ground motion accelerograms are

obtained from publications of the Geological Survey of Canada (Weichert et al. 1986, Munro and Weichert 1989, GSC 2006, Lin and Adams 2010) and the database of time-series from Southeastern Canada earthquakes available at <http://www.seisimotoolbox.ca> (last accessed July 2014). The AA13 central GMPE is selected as the reference GMPE to determine correlation coefficients in Eastern Canada. The difference between the 5%-damped acceleration spectra of the accelerograms considered and those predicted by AA13, i.e. ϵ , is then calculated at periods of between $T = 0.01$ s and $T = 5$ s. This definition of epsilon results in the same correlation coefficients as those obtained from the ϵ defined in Eq. (1) as also pointed out by Baker and Jayaram (2008). This definition will also introduce less bias in the results caused by the type of 5%-damped acceleration spectrum considered, e.g. geometric mean, individual component, or rotation independent geometric mean. The mean amplitudes for each type of 5%-damped acceleration spectrum are indeed very similar whereas this is not necessarily the case for corresponding standard deviations.

As suggested by Baker and Jayaram (2008), the Pearson product-moment correlation coefficient is used to estimate the correlation coefficient between $\epsilon(T_1)$ and $\epsilon(T_2)$, i.e. $\rho(T_1, T_2)$:

$$\rho(T_1, T_2) = \frac{\sum_{i=1}^n [\epsilon_i(T_1) - \overline{\epsilon(T_1)}] [\epsilon_i(T_2) - \overline{\epsilon(T_2)}]}{\sqrt{\sum_{i=1}^n [\epsilon_i(T_1) - \overline{\epsilon(T_1)}]^2 \sum_{i=1}^n [\epsilon_i(T_2) - \overline{\epsilon(T_2)}]^2}} \quad (6)$$

where n is the number of observations, i.e records, $\epsilon_i(T_1)$ and $\epsilon_i(T_2)$ are the i th observations of $\epsilon(T_1)$ and $\epsilon(T_2)$, respectively, and $\overline{\epsilon(T_1)}$ and $\overline{\epsilon(T_2)}$ are their means, respectively. Figs. 8 (a) and (b) show examples of calculated $\epsilon(T_1)$ and $\epsilon(T_2)$ values and the resulting $\rho(T_1, T_2)$, i.e. the slope of the illustrated lines. It can be seen that the $\rho(T_1, T_2)$ values, i.e. the slopes, for Eastern Canada are larger than those given by BJ08. This is confirmed through contour graphs for the $\rho(T_1, T_2)$ values corresponding to the majority of the period pairs obtained from Eq. (6) as illustrated in Figs. 9 (a) and (b). Although similar trends are observed in the obtained $\rho(T_1, T_2)$ from Eastern Canadian records and predictions of BJ08 model, the values are not identical. It seems that there is a higher correlation between spectral accelerations at different periods in Eastern Canada than predicted by BJ08 model. Carlton and Abrahamson (2014) suggest that correlation coefficients are sensitive to the high frequency content of ground motion records, e.g. those recorded on hard rock sites. Therefore, the application of correlation models such as BJ08 needs consideration of this characteristic of ground motions. Accordingly, Carlton and Abrahamson (2014) propose $T_{\text{amp}1.5}$, the shortest period at which $S_a(T)$ reaches 1.5 times the PGA, as a measure to determine the period at which the high frequency content influence the response spectrum. Carlton and Abrahamson (2014) report that the database of ground motions used to develop BJ08 has a $T_{\text{amp}1.5}$ of 0.1 s. They report that $\rho(T_1, T_2)$ values obtained from other data sets containing records from high seismicity regions and having $T_{\text{amp}1.5}$ close to that of BJ08 are very similar to predictions of BJ08.

Carlton and Abrahamson (2014) also propose that when BJ08 correlation coefficients are used to compute CMS from a controlling scenario (e.g. M and R scenarios) representing a response spectrum

that has a $T_{\text{amp}1.5}$ value different from 0.1 s, the following modifications be applied to obtain suitable BJ08 results: (i) determine $T^{*'} = 0.1 * T^*/T_{\text{amp}1.5}$; (ii) determine $\rho(T^{*'}, T)$ using BJ08 model; and (iii) calculate $T_{\text{new}} = T * T_{\text{amp}1.5}/0.1$. To investigate the applicability of the modified BJ08 correlation coefficients to Eastern Canada, first the $T_{\text{amp}1.5}$ of the records in the database of this study is calculated and found to be $T_{\text{amp}1.5} = 0.045$ s. This $T_{\text{amp}1.5} = 0.045$ s reveals the very high frequency characteristic of the Eastern Canadian records in comparison to those used to develop BJ08 model. The correlation coefficients from the database are then compared to those given by BJ08 model at different $T_{\text{amp}1.5}$ values. Both sets of coefficients, from Eastern Canada and from BJ08, are modified according to the procedure suggested by Carlton and Abrahamson (2014) where necessary. Figs. 10 and 11 illustrate the modified correlation coefficients, i.e. “Eastern Canada Modified” and “BJ08 Modified”, for $T^* = 0.2$ s, $T^* = 0.5$ s, $T^* = 1$ s, and $T^* = 2$ s. It can be seen that even after considering the effect of high frequency content of ground motions, the correlation coefficients obtained for Eastern Canada are higher than those predicted by BJ08 model. The observed shifts in the period ranges for the modified correlation coefficients result from conversion of their corresponding periods T to T_{new} which are not identical. It should be noted that the $\rho(T_1, T_2)$ values obtained from the historical records in Eastern Canada could be affected by the limitations associated with record selection in the region. We also note that the accelerograms included in the database compiled in this study were not used to develop AA13 GMPE, which is contrary to the approach adopted to develop BJ08 model. Based on the results presented in Figs. 10 and 11, there appears to be a need to further investigate the spectral correlations in this region in light of data recorded in the future.

4.2 Magnitude and distance dependence of correlation coefficients

Correlation coefficients from BJ08 model and those specific to Eastern Canada determined in this study both consider ρ to be independent from magnitude and distance of the ground motions. This is mainly based on the observations reported by Baker and Cornell (2005). To investigate the applicability of this assumption to ground motions in Eastern Canada, the accelerograms in the database are classified once based on the corresponding magnitude and then based on epicentral distance. Ground motions of magnitudes $M_W < 5$, which are more frequent in Eastern Canada (www.seismotoolbox.ca), are generally of lower importance for structural engineering purposes. Thus, records with magnitudes $M_W \geq 5$ and $M_W < 5$ are grouped together into bins M1 and M2, respectively, as indicated in Table 4. In addition, the accelerograms in the original database are divided into four bins based on epicentral distance R : (R1) $R \leq 100$ km, (R2) $100 \text{ km} < R \leq 200$ km, (R3) $200 \text{ km} < R \leq 400$ km, and (R4) $R \geq 400$ km. Ground motions with epicentral distances shorter than 100 km are generally more interesting for structural engineering applications. Therefore, records with distances in this range are grouped together in one bin, i.e. R1. Events with $100 \text{ km} < R \leq 200$ km can still have considerable effect on structures. As a result, the distance interval is kept at 100 km for the next bin, i.e. R2. This interval is increased to 200 km to form a bin from accelerograms recorded at longer distances less than 400 km, i.e. R3. As a number of GMPEs extend predictions to epicentral distances over 400 km (e.g. Atkinson and Adams 2011), ground motions recorded at such distances are also included and grouped together,

i.e. R4. The proposed distance-based classification of the accelerograms studied is presented in Table 5.

The correlation coefficients for each bin were next computed using AA13 central GMPE taking the same approach as in Section 4.1. The high frequency content of the records was also addressed by considering the $T_{\text{amp}1.5}$ corresponding to each bin and following the procedure suggested by Carlton and Abrahamson (2014). The values for $T_{\text{amp}1.5}$ corresponding to Bins M1 and M2 and Bins R1 to R4 were found to be 0.040 s, 0.047 s, 0.028 s, 0.042 s, 0.053 s and 0.063 s, respectively. Figs. 12 and 13 compare the obtained correlation coefficients to those determined regardless of magnitude and distance effects in Section 4.1 at $T^* = 0.2$ s, $T^* = 0.5$ s, $T^* = 1$ s, and $T^* = 2$ s. Figs. 12 and 13 clearly show that the period range through which the magnitude-dependency of correlation coefficients is pronounced, moves from longer periods to shorter periods as T^* increases. It is also illustrated that, in general, there is a higher correlation among the lower magnitude records in Eastern Canada, i.e. Bin M1. The correlation coefficients associated with the records from higher magnitudes, i.e. Bin M2, show a close agreement with those obtained from the entire database although the two sets tend to deviate at period ranges with high magnitude-dependency. This agreement can partly be related to the number of records in Bin M2 which contains approximately 2/3 of the records in the entire database. Figs. 14 and 15 reveal the distance-dependency of the correlation coefficients in Eastern Canada. It can be seen that the obtained distance-based correlation coefficients for Eastern Canada do not vary dramatically with epicentral distances up to 400 km, i.e. Bins R1, R2 and R3. Nevertheless, correlation coefficients of ground motions at very long distances, i.e. Bin R4, demonstrate poor correlation in the entire period range considered for almost all the values of T^* . In general, the difference between the coefficients from Bins R1, R2 and R3 and those from the entire database is mainly due to very low coefficients from Bin R4 which are considered in the determination of correlation coefficients for the entire database.

We next investigate whether the magnitude- and distance-based classifications of correlation coefficients computed for Eastern Canada will considerably affect the resulting CMS. To this end, the AA13 central GMPE is selected as the underlying model. The NBCC 2010 UHS for Toronto, Montreal and Quebec corresponding to NBCC 2010 site class A are adopted as the target spectra as all the ground motions studied were recorded on hard rock sites. The predictions of AA13 are modified to represent ground motions for site class A as already mentioned in Section 3.3. Modified correlation coefficients including the effects of high frequencies, i.e. $T_{\text{amp}1.5}$, are taken from the appropriate bins which are based on mean M and R from deaggregation, and are used to compute CMS. Figs. 16 to 21 present the computed CMS using the magnitude- and distance-based correlation coefficients along with the CMS computed using BJ08 correlation coefficients and those from the entire database of this study. It can be seen that, for all the three locations, magnitude-based coefficients do not have a considerable effect on the CMS when anchored at longer periods, i.e. $T = 1$ s and $T = 2$ s. However, when the CMS is anchored at shorter periods, i.e. $T = 0.2$ s and $T = 0.5$ s, higher spectral amplitudes are obtained using the magnitude-dependent coefficients.

As expected from the correlation coefficients illustrated in Figs. 10 and 11, adopting BJ08 model yields

to lower CMS in comparison to those using correlation coefficients obtained from the studied database of Eastern Canada records. Similar observations are made for the CMS constructed using distance-based coefficients. However, in this case the effect of distance is more pronounced when the CMS is anchored at longer periods. Generally, in comparison to the CMS computed using BJ08 model, it is seen that the obtained correlation coefficients result in higher spectral amplitudes at shorter period ranges. We also observe that, due to the modification made for the high frequency content of the records (Carlton and Abrahamson 2014), the period ranges through which the correlation coefficients are determined are modified based on the $T_{\text{amp}1.5}$ associated with each database of records. Hence, as can be seen in Figs. 16 to 21, the CMS obtained using BJ08 model and considering the $T_{\text{amp}1.5}$ for the controlling event, from deaggregation results, extends only up to $T = 1.7$ s. This is clearly seen in Figs. 10 and 11 when the coefficients are calculated for different values of $T_{\text{amp}1.5}$. This observation reiterates the necessity of further research to determine correlation models specific to Eastern Canada and underlines the possible underestimation when using BJ08 model to compute CMS in this region.

5 Conclusions

This work assessed the main ingredients required to construct CMS in Eastern Canada, and investigated the effect of their variations on the obtained CMS. The construction of CMS was reviewed and adapted to take account of the seismic hazard in three different Eastern Canadian cities: Toronto, Montreal and Quebec. The effect of variation in $\epsilon(T^*)$ on the computed CMS as a function of the underlying GMPE was investigated. It was shown that the selected GMPE can considerably affect the spectral amplitudes of the CMS mainly at shorter periods. This might have an impact on the seismic analysis or evaluation of structures with relatively short fundamental periods and also those for which higher mode effects are significant. The CMS computed using two approximate methods, i.e. “Methods 1 and 2” were found to be moderately different only at short period ranges. This is mainly due to the weights associated with the GMPEs for Eastern Canada. While “Method 1” could be used to compute CMS in Eastern Canada due to its simplicity, refined computations including logic tree weights are recommended for short-period structures or those significantly influenced by higher mode effects. We also investigated the applicability to Eastern Canada of spectral correlation models developed based on WNA ground motions. To this end, a database of ground motions recorded in Eastern Canada was compiled and correlation coefficients were determined using an up-to-date GMPE developed for ENA. The effects of higher frequency content of ground motions on correlation coefficients were also considered. The results suggest higher spectral correlations than predicted by a WNA-based model. We note however that this trend is based on currently available ground motions recorded in Eastern Canada and that it needs to be validated in light of future observations. Finally, we studied the dependency of correlation coefficients in Eastern Canada on magnitude and epicentral distance, two of the key characteristics of ground motions and their predictions. Records of lower magnitude demonstrated higher correlations at short periods for longer conditioning periods T^* . We found that the dependency of obtained correlation coefficients $\rho(T_1, T_2)$ on magnitude is generally pronounced as one of the two periods T_1 or T_2 is shifted towards the longer period range. Distance-dependency

was found to be less significant for distances of interest in structural engineering applications. We also showed that the effects of magnitude- or distance-based correlation coefficients on the CMS developed for the three cities are: (i) generally negligible at long periods, and (ii) significant at shorter periods particularly when the conditioning period T^* is less than approximately 0.5 s. This work is the first study addressing in detail the ingredients and construction of CMS in Eastern Canada. The methodology and results discussed are expected to enhance the application of CMS in this region.

Acknowledgements

The authors would like to acknowledge the financial support of the Natural Sciences and Engineering Research Council of Canada (NSERC), the Canadian Seismic Research Network (CSRN) and the Quebec Fund for Research on Nature and Technology (FRQNT).

References

- Abrahamson, N.A., and Silva, W.J. 2008. Summary of the Abrahamson & Silva NGA ground motion relations. *Earthquake Spectra*, **24**: 67–97.
- Atkinson, G.M. 2008. Ground-motion prediction equations for Eastern North America from a referenced empirical approach: Implications for epistemic uncertainty. *Bulletin of the Seismological Society of America*, **98**(3): 1304–1318.
- Atkinson, G.M., and Adams, J. 2013. Ground motion prediction equations for application to the 2015 Canadian national seismic hazard maps. *Canadian Journal of Civil Engineering*, **40**: 988–998.
- Atkinson, G.M., and Boore, D.M. 2006. Earthquake ground-motion prediction equations for eastern north America. *Bulletin of the Seismological Society of America*, **96**(6): 2181–2205.
- Atkinson, G.M., and Boore, D.M. 2011. Modifications to existing ground-motion prediction equations in light of new data. *Bulletin of the Seismological Society of America*, **101**(3): 1121–1135.
- Baker, J.W. 2011. Conditional Mean Spectrum: tool for ground-motion selection. *Journal of Structural Engineering*, **137**(3): 322–331.
- Baker, J.W., and Cornell, C.A. 2005. Vector-valued ground motion intensity measure for probabilistic seismic demand analysis. John A. Blume Earthquake Engineering Center, Report No. 150, Stanford, California.
- Baker, J.W., and Cornell, C.A. 2006. Correlation of response spectral values for multi-component ground motions. *Bulletin of the Seismological Society of America*, **96**(1): 215–227.
- Baker, J.W, and Jayaram, N. 2008. Correlation of spectral acceleration values from NGA ground motion models. *Earthquake Spectra*, **24**(1): 299–317.
- Boore, D.M. 1983. Stochastic simulation of high-frequency ground motions based on seismological models of the radiated spectra, **73**: 1865–1894.
- Boore, D.M., and Atkinson, G.M. 2008. Ground-motion prediction equations for the average horizontal component of PGA, PGV, and 5%-damped PSA at spectral periods between 0.01 s and 10.0 s. *Earthquake Spectra*, **24**(1): 99–138.
- Burks, L.S., Baker, J.W. 2012. Occurrence of negative epsilon in seismic hazard analysis deaggregation, and its impact on target spectra computation. *Earthquake Engineering and Structural Dynamics*, **41**(8): 1241–1256.
- Campbell, K.W. 2003. Prediction of strong motion using the hybrid empirical method and its use in the development of ground-motion (attenuation) relations in Eastern North America. *Bulletin of the Seismological Society of America*, **93**(3): 1012–1033.
- Campbell, K.W., and Bozorgnia, Y. 2008. NGA ground motion model for the geometric mean horizontal component of PGA, PGV, PGD and 5% damped linear elastic response spectra for periods ranging from 0.01 to 10 s. *Earthquake Spectra*, **24**: 139–171.
- Carlton, B., and Abrahamson, N. 2014. Issues and approaches for implementing conditional mean spectra in practice. *Bulletin of the Seismological Society of America*, **104**(1): 503–512.

- Chiou, B.S.J., and Youngs, R.R. 2008. An NGA model for the average horizontal component of peak ground motion and response spectra. *Earthquake Spectra*, **24**(3): 173–215.
- Daneshvar, P., Bouaanani N., and Leger, P. 2014. application of conditional mean spectra for evaluation of a building's seismic response in Eastern Canada. *Canadian Journal of Civil Engineering*, **41**(8): 769–773.
- Hanks, T., and McGuire, R.K. 1981. The character of high-frequency strong ground motion. *Bulletin of the Seismological Society of America*, **71**: 2071–2095.
- Harmsen, S.C. 2001. Mean and modal epsilon in the deaggregation of probabilistic ground motion. *Bulletin of the Seismological Society of America*, **91**(6): 1537–1552.
- Idriss, I.M. 2008. An NGA empirical model for estimating the horizontal spectral values generated by shallow crustal earthquakes. *Earthquake Spectra*, **24**: 217–242.
- Inoue, T., and Cornell, C.A. 1990. Seismic hazard analysis of multi-degree-of-freedom structures. *Reliability of Marine Structures, RMS-8*, Stanford, CA, 70 pp.
- Jayaram, N., Baker, J.W., Okano, H., Ishida, H., McCann, M.W. and Mihara, Y. 2011. Correlation of response spectral values in Japanese ground motions. *Earthquakes and Structures*, **2**(4): 357–376.
- Lin, L., Adams, J. 2010. Strong motion records of the Val-des-Bois, Québec, Earthquake of June 23, 2010. Canadian Hazard Information Service Internal Report 2010-1.1, Geological Survey of Canada.
- Lin, T., Harmsen S.C., Baker, J.W., and Luco, N. 2013. Conditional Spectrum computation incorporating multiple causal earthquakes and ground motion prediction models. *Bulletin of the Seismological Society of America*, **103**(2A): 1103–1116.
- McGuire, R.K. 1995. Probabilistic seismic hazard analysis and design earthquakes: closing the loop. *Bulletin of the Seismological Society of America* **85**(5): 1275–1284.
- Munro, P.S., and Weichert, D. 1989. The Saguenay earthquake of November 25, 1988, Processed strong motion records. Geological Survey of Canada, Open File 1996.
- NBCC. 2010. National Building Code of Canada, Associate Committee on the National Building Code, National Research Council of Canada, Ottawa, Ont.
- Pezeshk, S., Zandieh, A., and Tavakoli, B. 2011. Hybrid empirical ground-motion prediction equations for Eastern North America using NGA models and updated seismological parameters. *Bulletin of the Seismological Society of America*, **101**(4): 1859–1870.
- Silva, W., Gregor, N., and Darragh, R. 2002. Development of regional hard rock attenuation relations for Central and Eastern North America. Technical Report, Pacific Engineering and Analysis, El Cerrito, California.
- Weichert, D.H., Wetmiller, R.J., Horner, R.B., Munro, P.S. and Mork, P.N. 1986. Strong Motion Records from the 23 December 1985, Ms 6.9 Nahanni, NWT, and some Associated Earthquakes. Geological Survey of Canada, Pacific Geoscience Centre, Open File Report 1330.

List of tables

Tab. 1: Characteristics of the ground motion prediction equations used in this study.

Tab. 2: Mean magnitude and distance scenarios for Toronto, Montreal and Quebec at different periods extracted from deaggregation results (GSC 2010).

Tab. 3: Historical ENA ground motions studied.

Tab. 4: Magnitude-based classification of the records in the studied database of ground motions.

Tab. 5: Distance-based classification of the records in the studied database of ground motions.

Table 1: Characteristics of the ground motion prediction equations used in this study.

GMPEs	Mag. scale/Range	Dist. metric/Range	Period range	Response variables	Damping values
Silva et al. (2002) - SGD02	$M_W/4.5 - 8.5$	$R_{jb}/ 1 - 400 \text{ km}$	0 - 10 s	PSA	5%
Atkinson and Boore (2006) - AB06	$M_W/3.5 - 8.0$	$R_{RUP}/ 1 - 1000 \text{ km}$	0 - 5 s	PSA	5%
Atkinson (2008) - A08	$M_W/4.3 - 7.6$	$R_{jb}/ 1 - 1000 \text{ km}$	0 - 5 s	PSA	5%
Pezeshk et al. (2011) - PZT11	$M_W/5.0 - 8.0$	$R_{RUP}/ 1 - 1000 \text{ km}$	0 - 10 s	PSA	5%
Atkinson and Adams (2013) - AA13	$M_W/4.5 - 8.0$	$R_{EPI}/ 1 - 800 \text{ km}$	0 - 10 s	PSA	5%

Table 2

Mean magnitude and distance scenarios for Toronto, Montreal and Quebec at different periods extracted from deaggregation results (GSC 2010).

Location	T (s)	M_W	R (km)
Toronto	0.2	5.6	99
	0.5	6.4	217
	1.0	6.7	234
	2.0	6.8	282
Montreal	0.2	6.1	36
	0.5	6.6	51
	1.0	6.8	64
	2.0	6.9	79
Quebec	0.2	6.0	41
	0.5	6.6	68
	1.0	6.8	81
	2.0	6.8	95

Table 3
Historical ENA ground motions studied.

Event	M_W	Number of Records	Site Class
Nahanni (11/1985)	4.6	2	A
Nahanni (12/1985)	6.9	4	A
Saguenay (1988)	5.8	18	A
Cap-Rouge (1997)	4.7	16	A
Pymatuning (1998)	5.0	2	A
Côte-Nord (1999)	4.7	18	A
Au-Sable-Forks (2002)	5.1	26	A
Rivière-du-Loup (2005)	5.0	16	A
Val-des-Bois (2010)	5.0	6	A

Table 4

Magnitude-based classification of the records in the studied database of ground motions.

Bin	Event	M_W	Number of Records
M1	Nahanni (12/1985)	6.9	4
	Saguenay (1988)	5.8	18
	Pymatuning (1998)	5.0	2
	Au-Sable-Forks (2002)	5.1	26
	Rivière-du-Loup (2005)	5.0	16
	Val-des-Bois (2010)	5.0	6
M2	Nahanni (11/1985)	4.6	2
	Cap-Rouge (1997)	4.7	16
	Côte-Nord (1999)	4.7	18

Table 5

Distance-based classification of the records in the studied database of ground motions.

Event	M_W	R1	R2	R3	R4
Nahanni (11/1985)	4.6	2	–	–	–
Nahanni (12/1985)	6.9	4	–	–	–
Saguenay (1988)	5.8	8	10	–	–
Cap-Rouge (1997)	4.7	–	12	2	2
Pymatuning (1998)	5.0	–	–	2	–
Côte-Nord (1999)	4.7	–	–	14	4
Au-Sable-Forks (2002)	5.1	–	4	2	20
Rivière-du-Loup (2005)	5.0	14	–	2	–
Val-des-Bois (2010)	5.0	6	–	–	–

List of figures

- Fig. 1: Flowchart illustrating the procedure to compute CMS.
- Fig. 2: GMPE-based variation of CMS computed by matching to NBCC 2010 prescribed UHS for Toronto at: (a) $T^* = 0.2$ s, (b) $T^* = 0.5$ s, (c) $T^* = 1$ s, and (d) $T^* = 2$ s.
- Fig. 3: GMPE-based variation of CMS computed by matching to NBCC 2010 prescribed UHS for Montreal at: (a) $T^* = 0.2$ s, (b) $T^* = 0.5$ s, (c) $T^* = 1$ s, and (d) $T^* = 2$ s.
- Fig. 4: GMPE-based variation of CMS computed by matching to NBCC 2010 prescribed UHS for Quebec at: (a) $T^* = 0.2$ s, (b) $T^* = 0.5$ s, (c) $T^* = 1$ s, and (d) $T^* = 2$ s.
- Fig. 5: CMS computed using Method 2 (Lin et al. 2013) and by matching to NBCC 2010 prescribed UHS for Toronto at: (a) $T^* = 0.2$ s, (b) $T^* = 0.5$ s, (c) $T^* = 1$ s, and (d) $T^* = 2$ s compared to CMS computed using single GMPE.
- Fig. 6: CMS computed using Method 2 (Lin et al. 2013) and by matching to NBCC 2010 prescribed UHS for Montreal at: (a) $T^* = 0.2$ s, (b) $T^* = 0.5$ s, (c) $T^* = 1$ s, and (d) $T^* = 2$ s compared to CMS computed using single GMPE.
- Fig. 7: CMS computed using Method 2 (Lin et al. 2013) and by matching to NBCC 2010 prescribed UHS for Quebec at: (a) $T^* = 0.2$ s, (b) $T^* = 0.5$ s, (c) $T^* = 1$ s, and (d) $T^* = 2$ s compared to CMS computed using single GMPE.
- Fig. 8: Observed $\epsilon(T)$ and the corresponding correlation coefficients: (a) between $T = 0.5$ s and $T = 1$ s, and (b) between $T = 1$ s and $T = 2$ s.
- Fig. 9: Correlation coefficients obtained from: (a) ground motions in Eastern Canada, and (b) Baker and Jayaram (2008). The numbers over the contour lines represent the corresponding correlation coefficients.
- Fig. 10: Comparison between obtained correlation coefficients for Eastern Canada and those from BJ08 model at different $T_{\text{amp}1.5}$ values for: (a) $T^* = 0.2$ s, and (b) $T^* = 0.5$ s.
- Fig. 11: Comparison between obtained correlation coefficients for Eastern Canada and those from BJ08 model at different $T_{\text{amp}1.5}$ values for: (a) $T^* = 1$ s, and (b) $T^* = 2$ s.
- Fig. 12: Comparison between obtained correlation coefficients for Eastern Canada from magnitude-based bins and those from the entire records database at different $T_{\text{amp}1.5}$ values for: (a) $T^* = 0.2$ s, and (b) $T^* = 0.5$ s.
- Fig. 13: Comparison between obtained correlation coefficients for Eastern Canada from magnitude-based bins and those from the entire records database at different $T_{\text{amp}1.5}$ values for: (a) $T^* = 1$ s, and (b) $T^* = 2$ s.
- Fig. 14: Comparison between obtained correlation coefficients for Eastern Canada from distance-based bins and those from the entire records database at different $T_{\text{amp}1.5}$ values for: (a) $T^* = 0.2$ s, and (b) $T^* = 0.5$ s.
- Fig. 15: Comparison between obtained correlation coefficients for Eastern Canada from distance-based bins and those from the entire records database at different $T_{\text{amp}1.5}$ values for: (a) $T^* = 0.2$ s, and (b) $T^* = 0.5$ s.
- Fig. 16: CMS computed using magnitude-based ρ s for Eastern Canada and by matching to NBCC 2010 prescribed UHS for Toronto at: (a) $T^* = 0.2$ s, (b) $T^* = 0.5$ s, (c) $T^* = 1$ s, and (d) $T^* = 2$ s.
- Fig. 17: CMS computed using magnitude-based ρ s for Eastern Canada and by matching to NBCC 2010

prescribed UHS for Montreal at: (a) $T^* = 0.2$ s, (b) $T^* = 0.5$ s, (c) $T^* = 1$ s, and (d) $T^* = 2$ s.

Fig. 18: CMS computed using magnitude-based ρ s for Eastern Canada and by matching to NBCC 2010 prescribed UHS for Quebec at: (a) $T^* = 0.2$ s, (b) $T^* = 0.5$ s, (c) $T^* = 1$ s, and (d) $T^* = 2$ s.

Fig. 19: CMS computed using distance-based ρ s for Eastern Canada and by matching to NBCC 2010 prescribed UHS for Toronto at: (a) $T^* = 0.2$ s, (b) $T^* = 0.5$ s, (c) $T^* = 1$ s, and (d) $T^* = 2$ s.

Fig. 20: CMS computed using distance-based ρ s for Eastern Canada and by matching to NBCC 2010 prescribed UHS for Montreal at: (a) $T^* = 0.2$ s, (b) $T^* = 0.5$ s, (c) $T^* = 1$ s, and (d) $T^* = 2$ s.

Fig. 21: CMS computed using distance-based ρ s for Eastern Canada and by matching to NBCC 2010 prescribed UHS for Quebec at: (a) $T^* = 0.2$ s, (b) $T^* = 0.5$ s, (c) $T^* = 1$ s, and (d) $T^* = 2$ s.

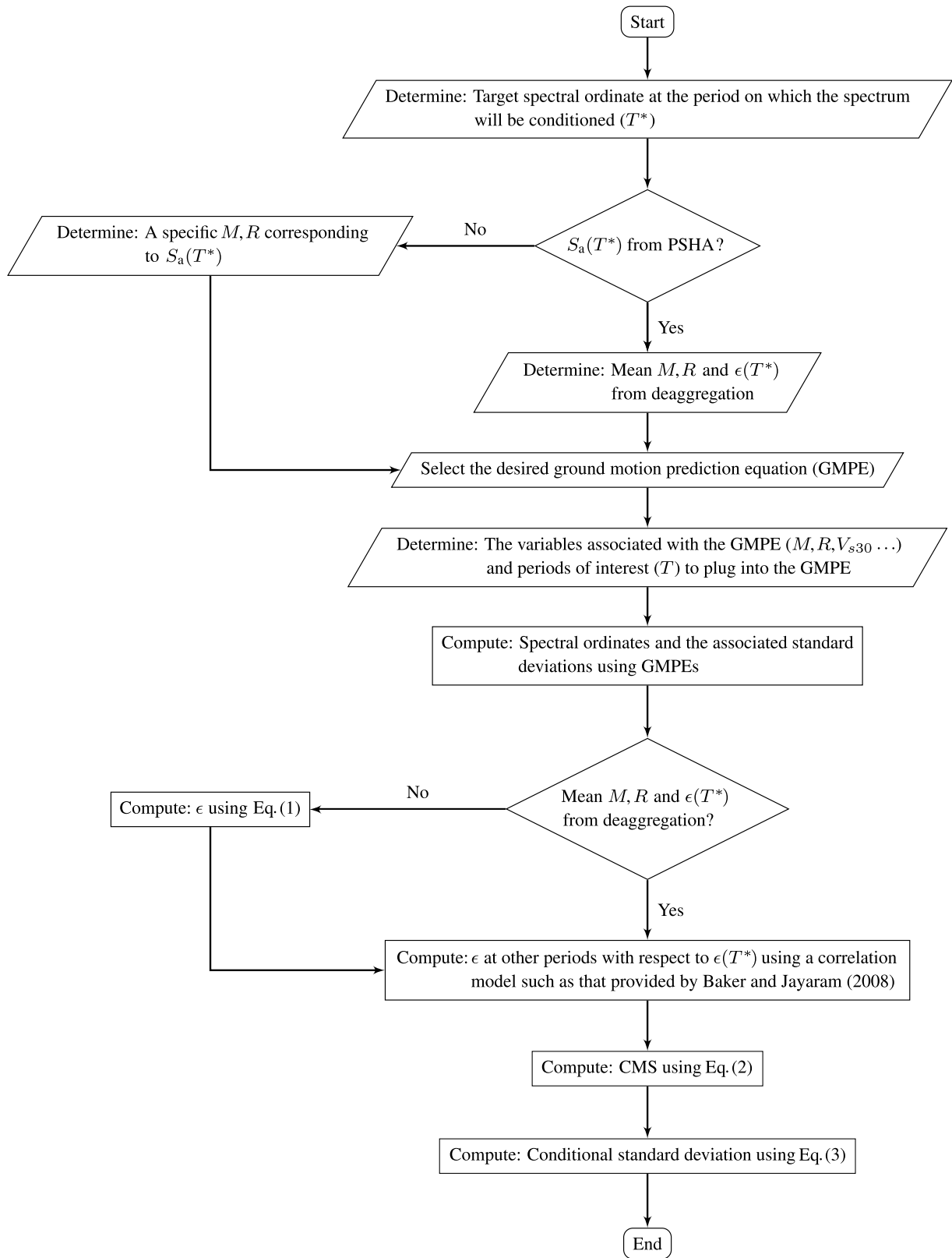


Figure 1. Flowchart illustrating the procedure to compute CMS.

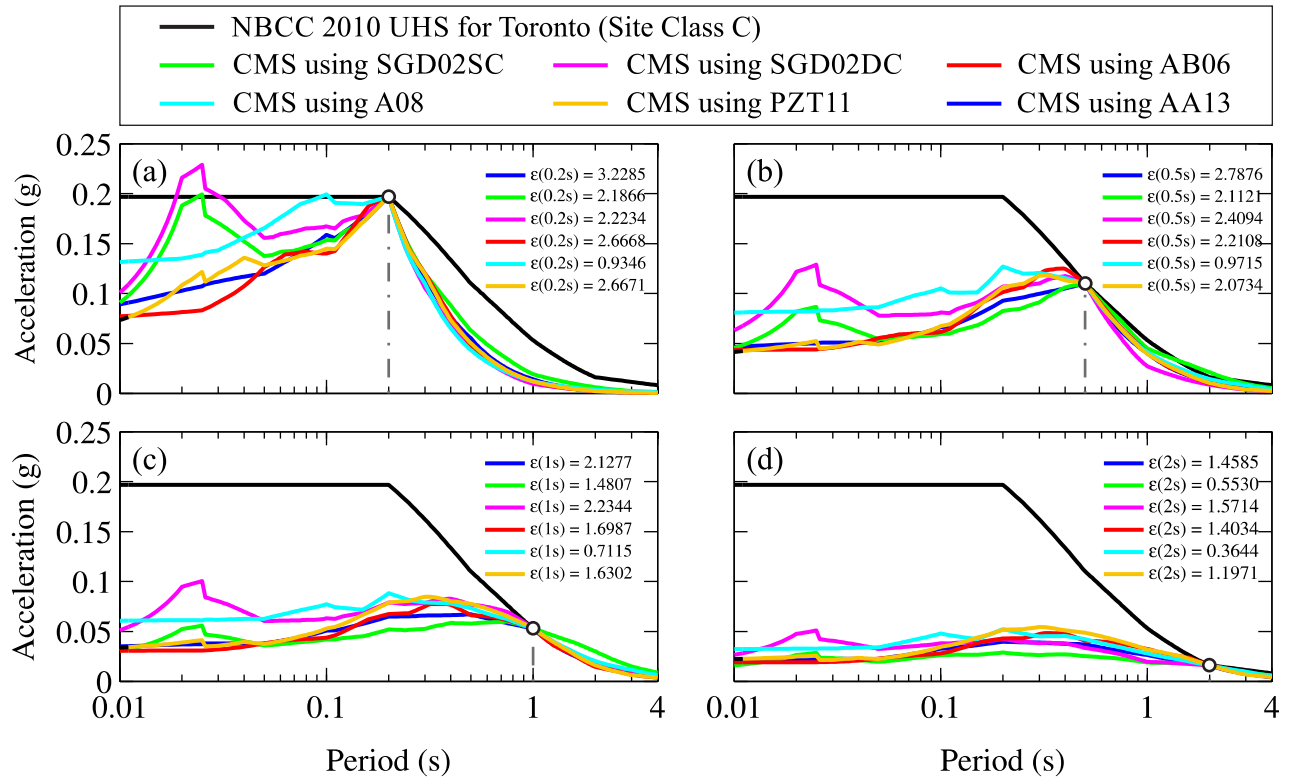


Figure 2. GMPE-based variation of CMS computed by matching to NBCC 2010 prescribed UHS for Toronto at: (a) $T^* = 0.2$ s, (b) $T^* = 0.5$ s, (c) $T^* = 1$ s, and (d) $T^* = 2$ s.

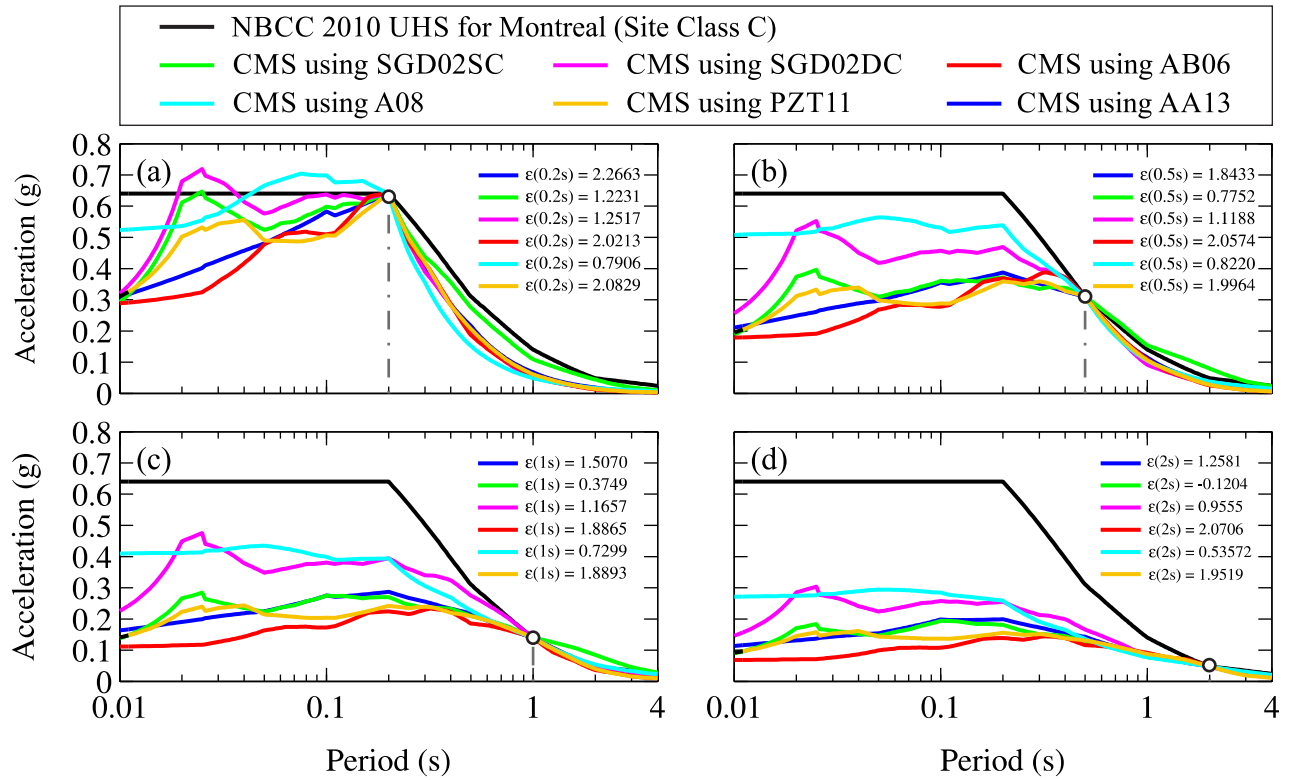


Figure 3. GMPE-based variation of CMS computed by matching to NBCC 2010 prescribed UHS for Montreal at: (a) $T^* = 0.2$ s, (b) $T^* = 0.5$ s, (c) $T^* = 1$ s, and (d) $T^* = 2$ s.

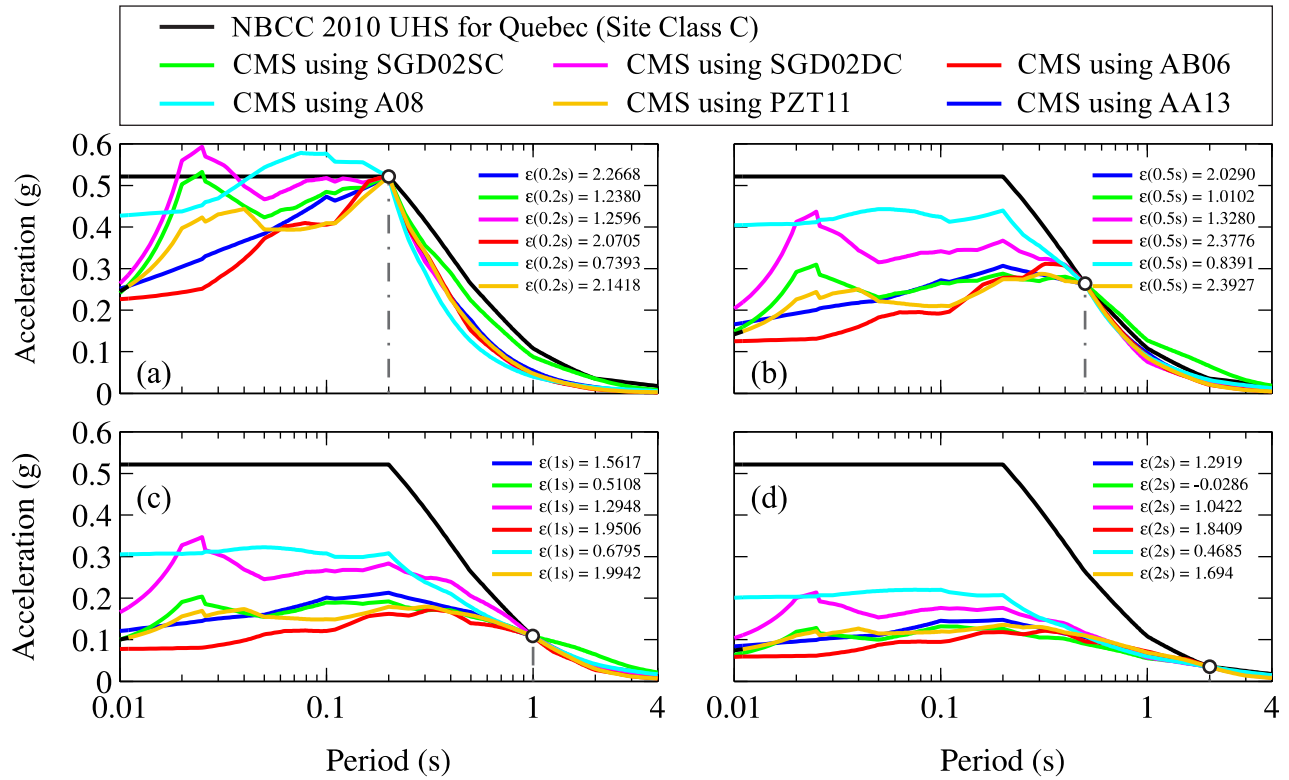


Figure 4. GMPE-based variation of CMS computed by matching to NBCC 2010 prescribed UHS for Quebec at: (a) $T^* = 0.2$ s, (b) $T^* = 0.5$ s, (c) $T^* = 1$ s, and (d) $T^* = 2$ s.

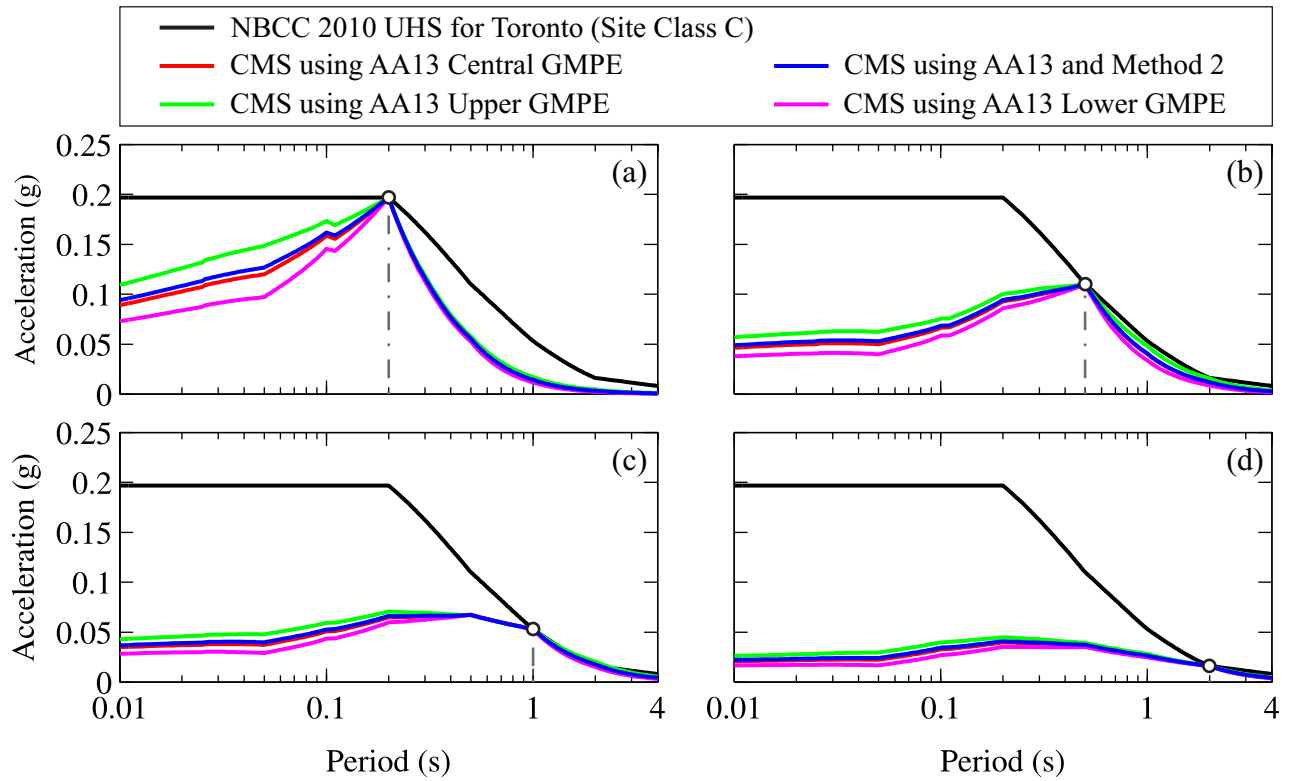


Figure 5. CMS computed using Method 2 (Lin et al. 2013) and by matching to NBCC 2010 prescribed UHS for Toronto at: (a) $T^* = 0.2$ s, (b) $T^* = 0.5$ s, (c) $T^* = 1$ s, and (d) $T^* = 2$ s compared to CMS computed using single GMPE.

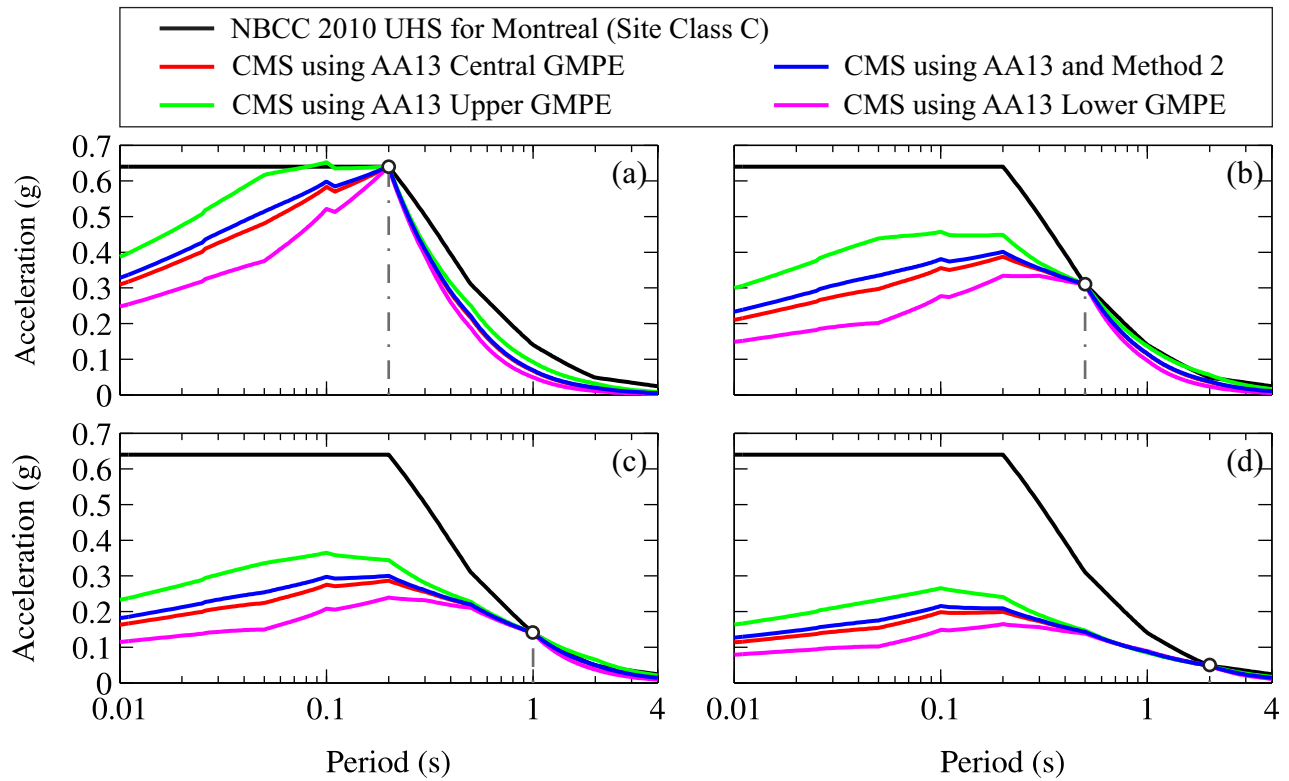


Figure 6. CMS computed using Method 2 (Lin et al. 2013) and by matching to NBCC 2010 prescribed UHS for Montreal at: (a) $T^* = 0.2$ s, (b) $T^* = 0.5$ s, (c) $T^* = 1$ s, and (d) $T^* = 2$ s compared to CMS computed using single GMPE.

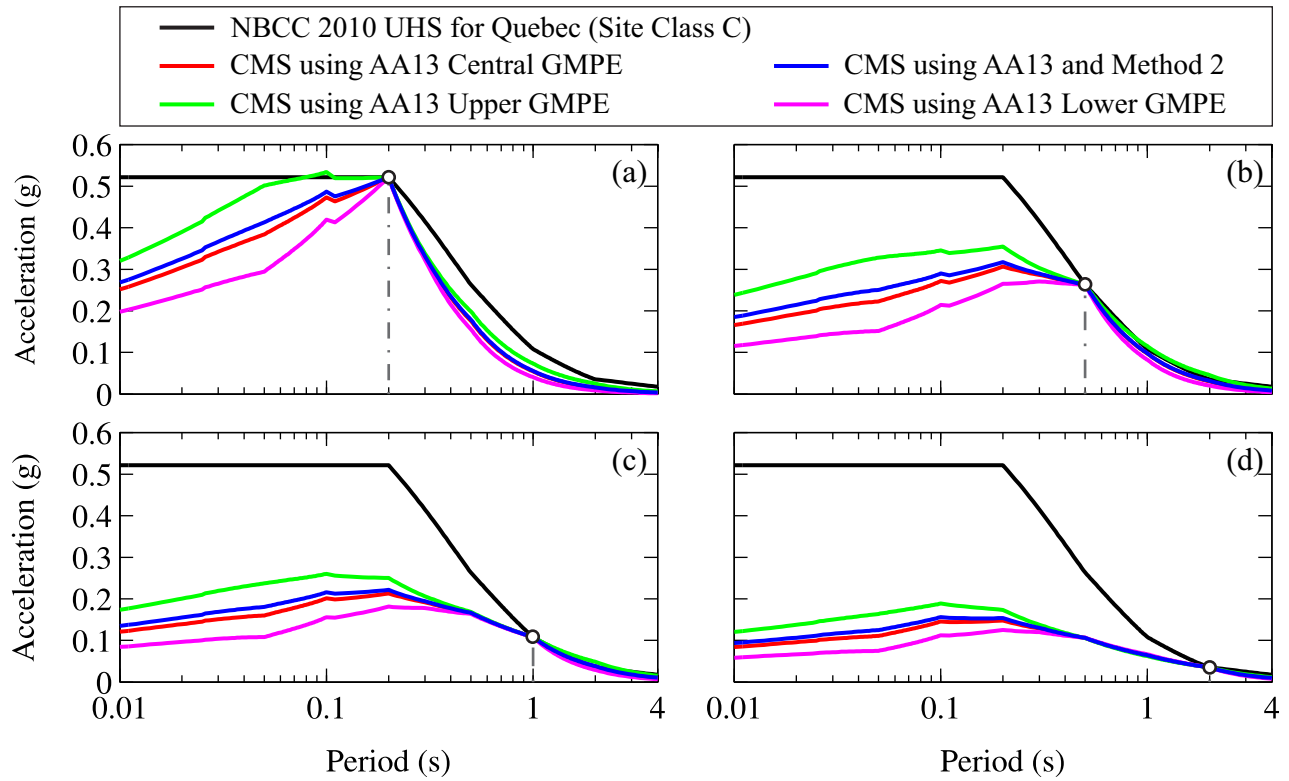


Figure 7. CMS computed using Method 2 (Lin et al. 2013) and by matching to NBCC 2010 prescribed UHS for Quebec at: (a) $T^* = 0.2$ s, (b) $T^* = 0.5$ s, (c) $T^* = 1$ s, and (d) $T^* = 2$ s compared to CMS computed using single GMPE.

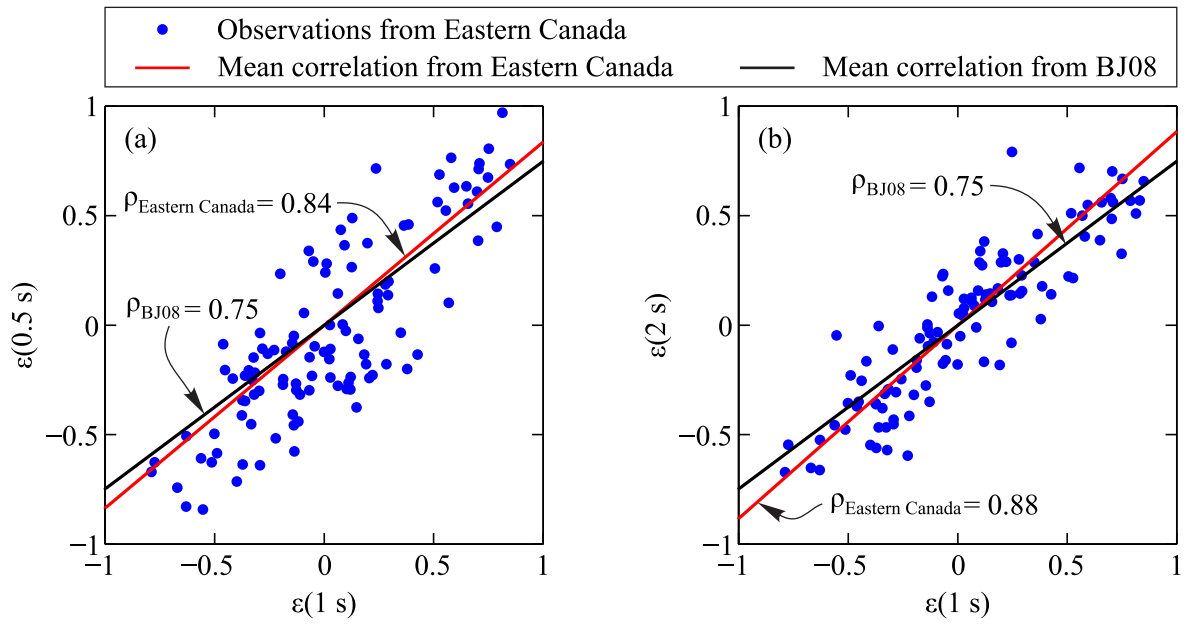


Figure 8. Observed $\epsilon(T)$ and the corresponding correlation coefficients defined as the slope of each line: (a) between $T=0.5 \text{ s}$ and $T=1 \text{ s}$, and (b) between $T=1 \text{ s}$ and $T=2 \text{ s}$.

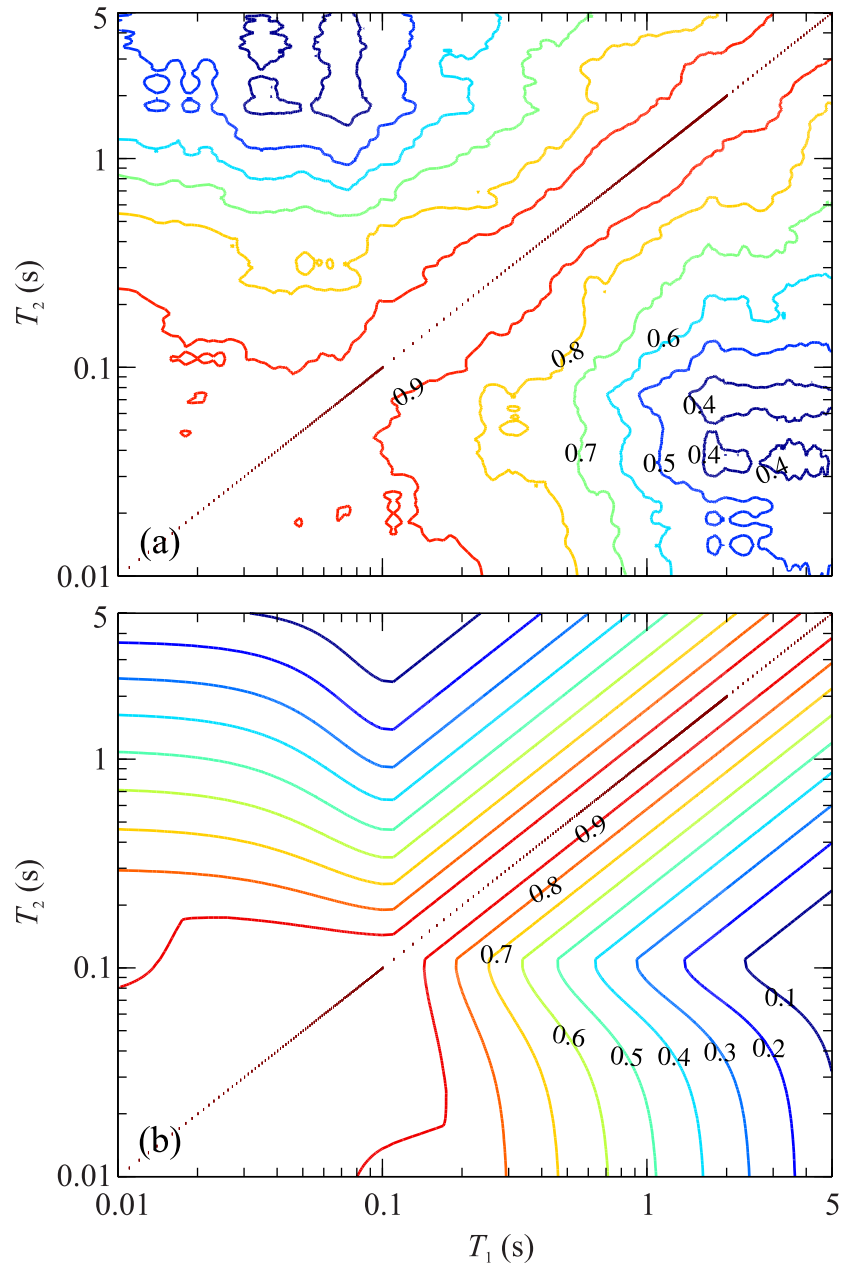


Figure 9. Correlation coefficients obtained from: (a) ground motions in Eastern Canada, and (b) Baker and Jayaram (2008). The numbers over the contour lines represent the corresponding correlation coefficients.

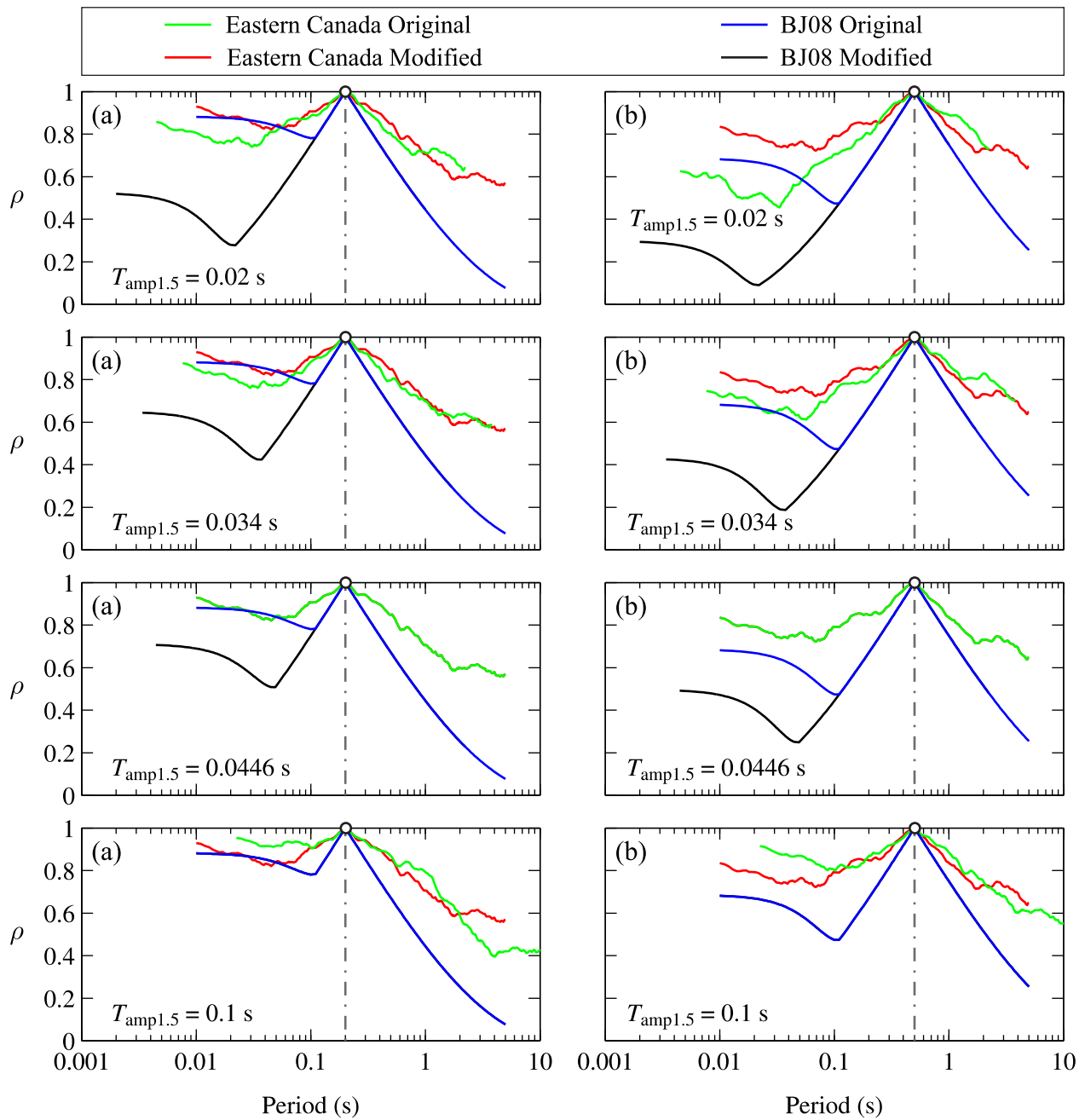


Figure 10. Comparison between obtained correlation coefficients for Eastern Canada and those from BJ08 model at different $T_{\text{amp}1.5}$ values for: (a) $T^* = 0.2$ s, and (b) $T^* = 0.5$ s.

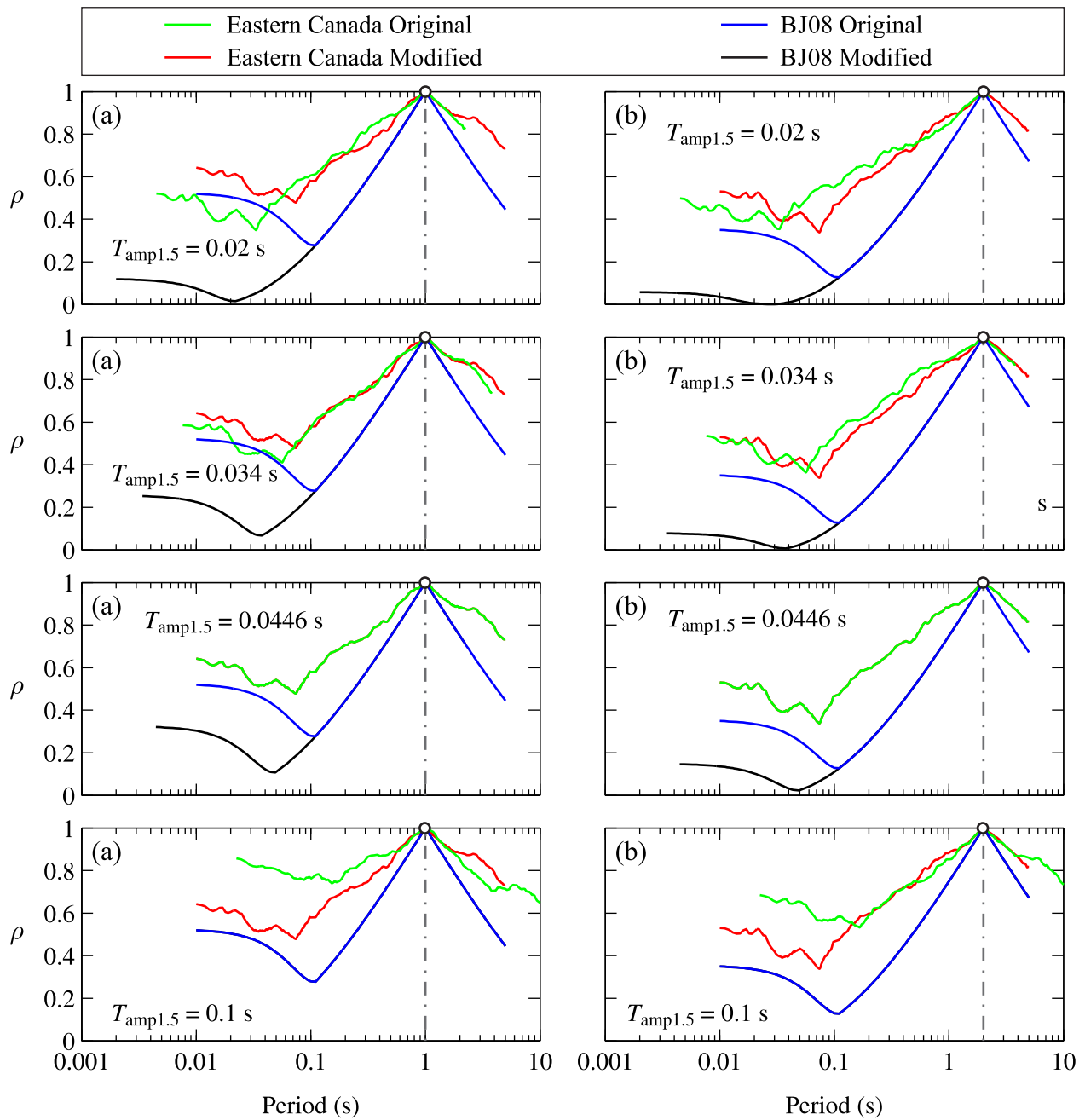


Figure 11. Comparison between obtained correlation coefficients for Eastern Canada and those from BJ08 model at different $T_{amp1.5}$ values for: (a) $T^* = 1$ s, and (b) $T^* = 2$ s.

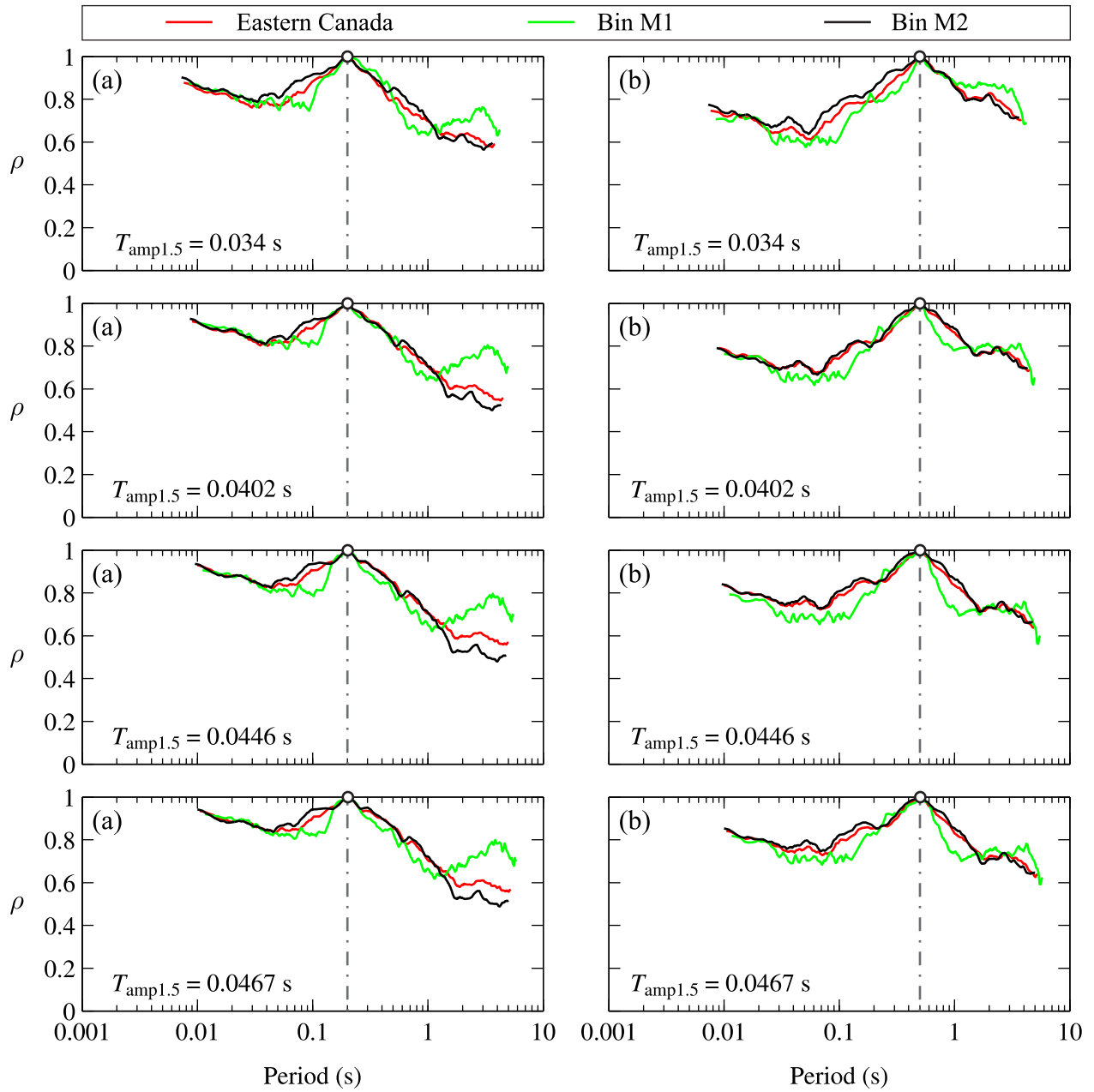


Figure 12. Comparison between obtained correlation coefficients for Eastern Canada from magnitude-based bins and those from the entire records database at different $T_{amp1.5}$ values for: (a) $T^* = 0.2$ s, and (b) $T^* = 0.5$ s.

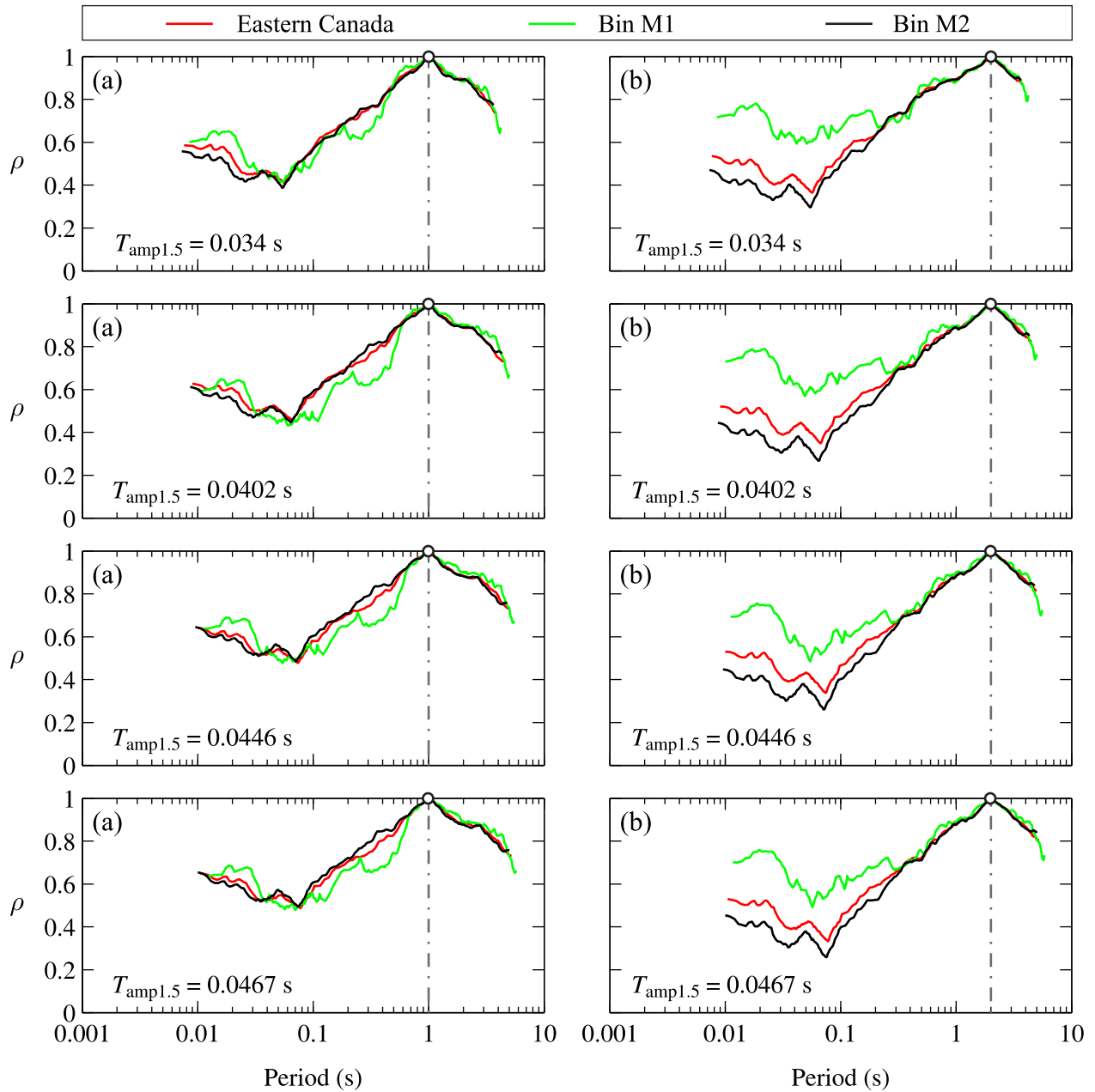


Figure 13. Comparison between obtained correlation coefficients for Eastern Canada from magnitude-based bins and those from the entire records database at different $T_{\text{amp}1.5}$ values for: (a) $T^* = 1$ s, and (b) $T^* = 2$ s.

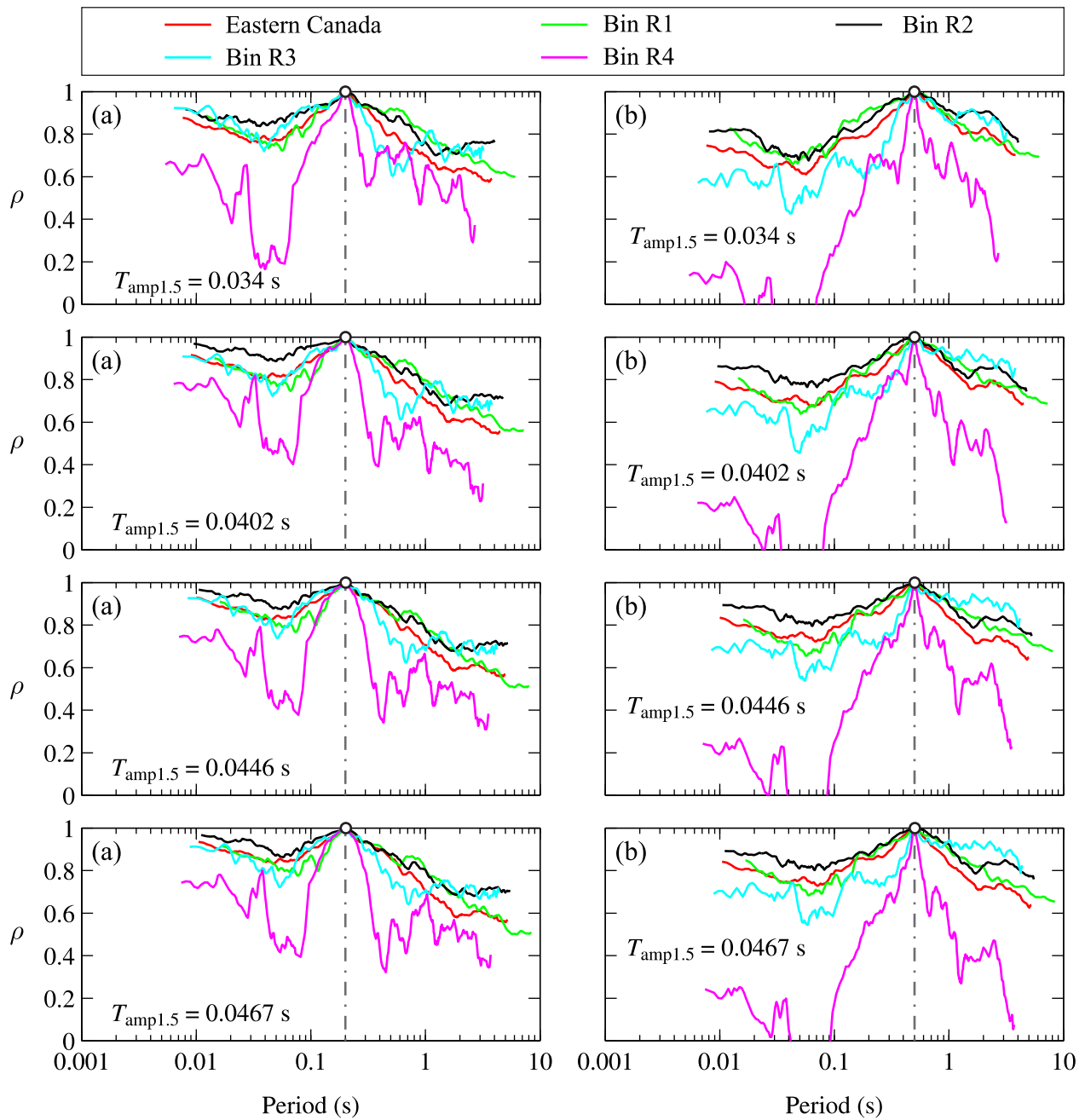


Figure 14. Comparison between obtained correlation coefficients for Eastern Canada from distance-based bins and those from the entire records database at different $T_{amp1.5}$ values for: (a) $T^* = 0.2$ s, and (b) $T^* = 0.5$ s.

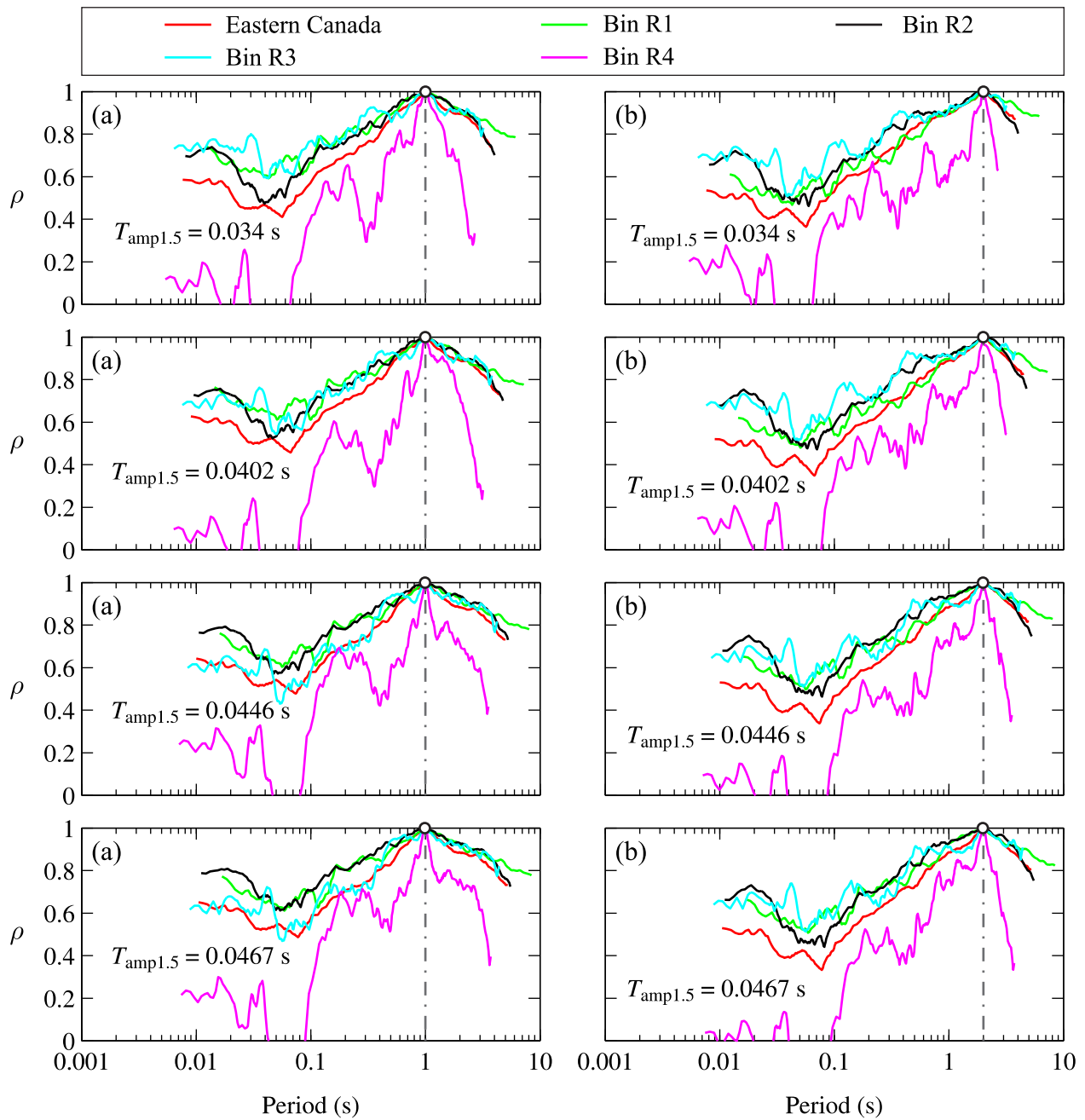


Figure 15. Comparison between obtained correlation coefficients for Eastern Canada from distance-based bins and those from the entire records database at different $T_{amp1.5}$ values for: (a) $T^* = 0.2$ s, and (b) $T^* = 0.5$ s.

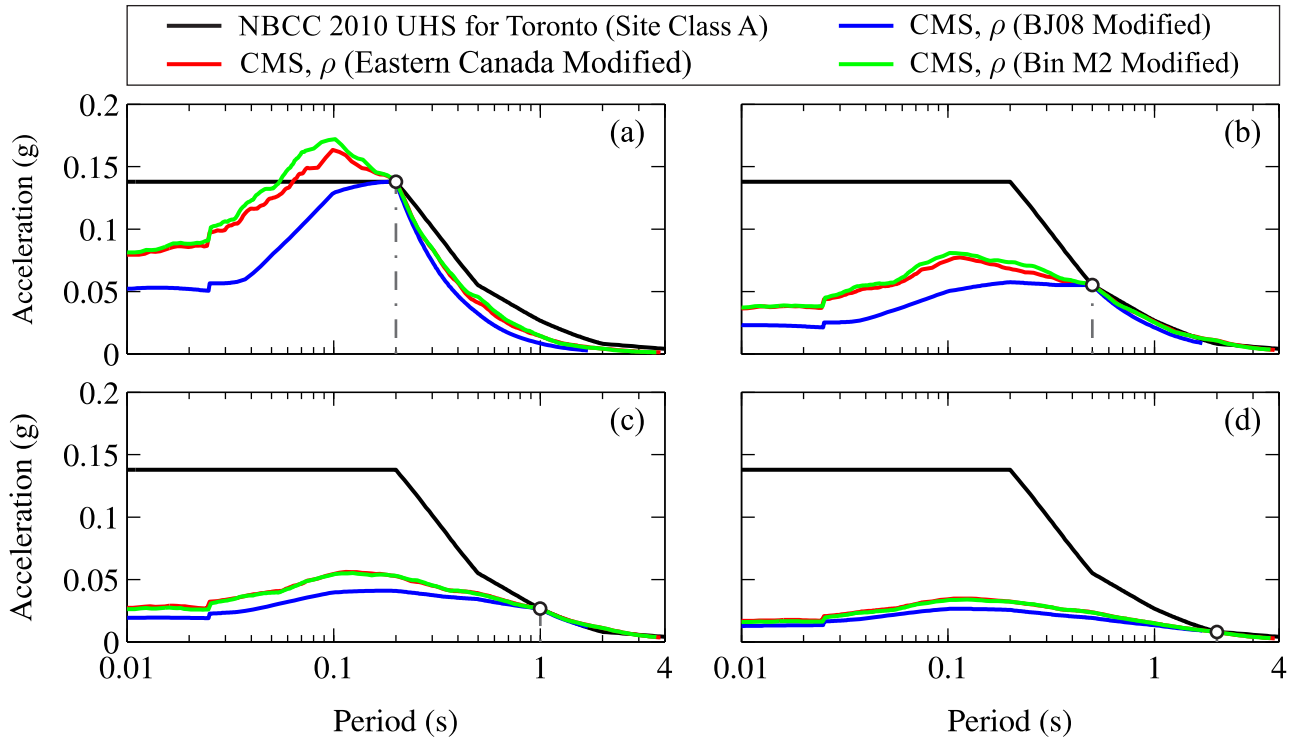


Figure 16. CMS computed using magnitude-based ρ s for Eastern Canada and by matching to NBCC 2010 prescribed UHS for Toronto at: (a) $T^* = 0.2$ s, (b) $T^* = 0.5$ s, (c) $T^* = 1$ s, and (d) $T^* = 2$ s.

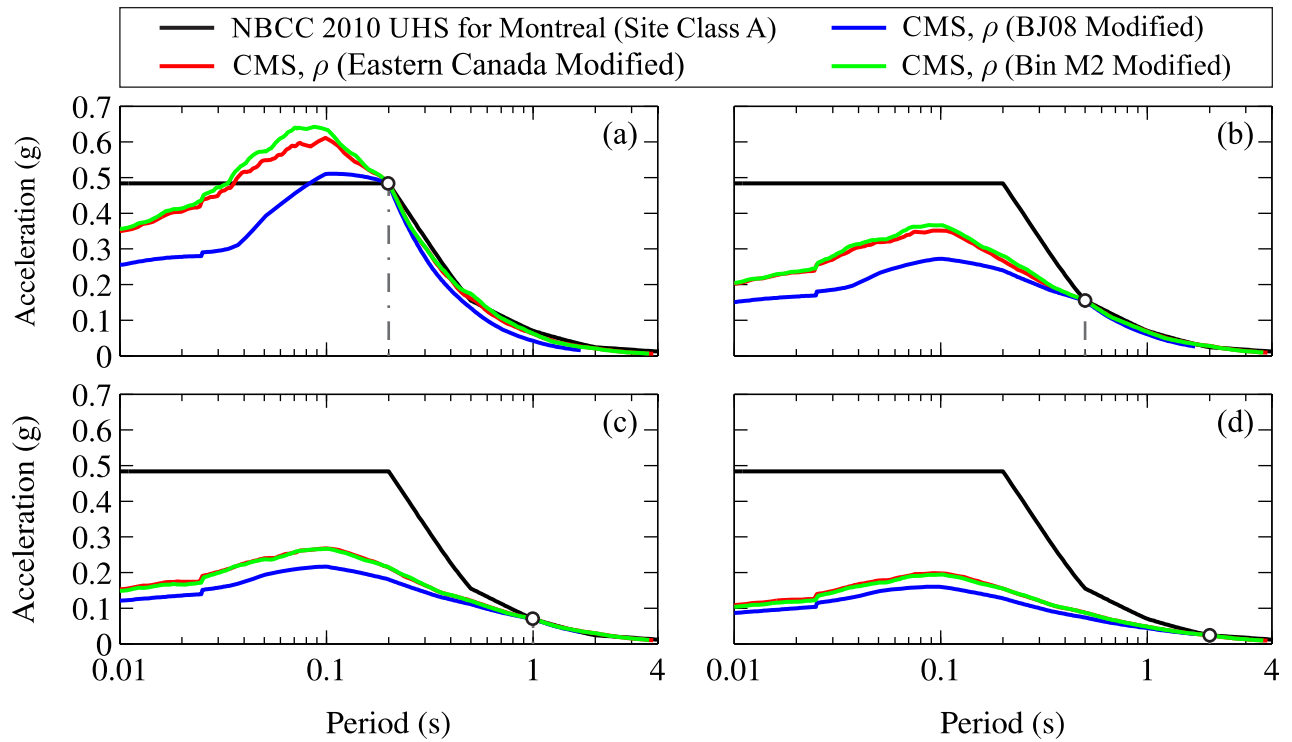


Figure 17. CMS computed using magnitude-based ρ s for Eastern Canada and by matching to NBCC 2010 prescribed UHS for Montreal at: (a) $T^* = 0.2$ s, (b) $T^* = 0.5$ s, (c) $T^* = 1$ s, and (d) $T^* = 2$ s.

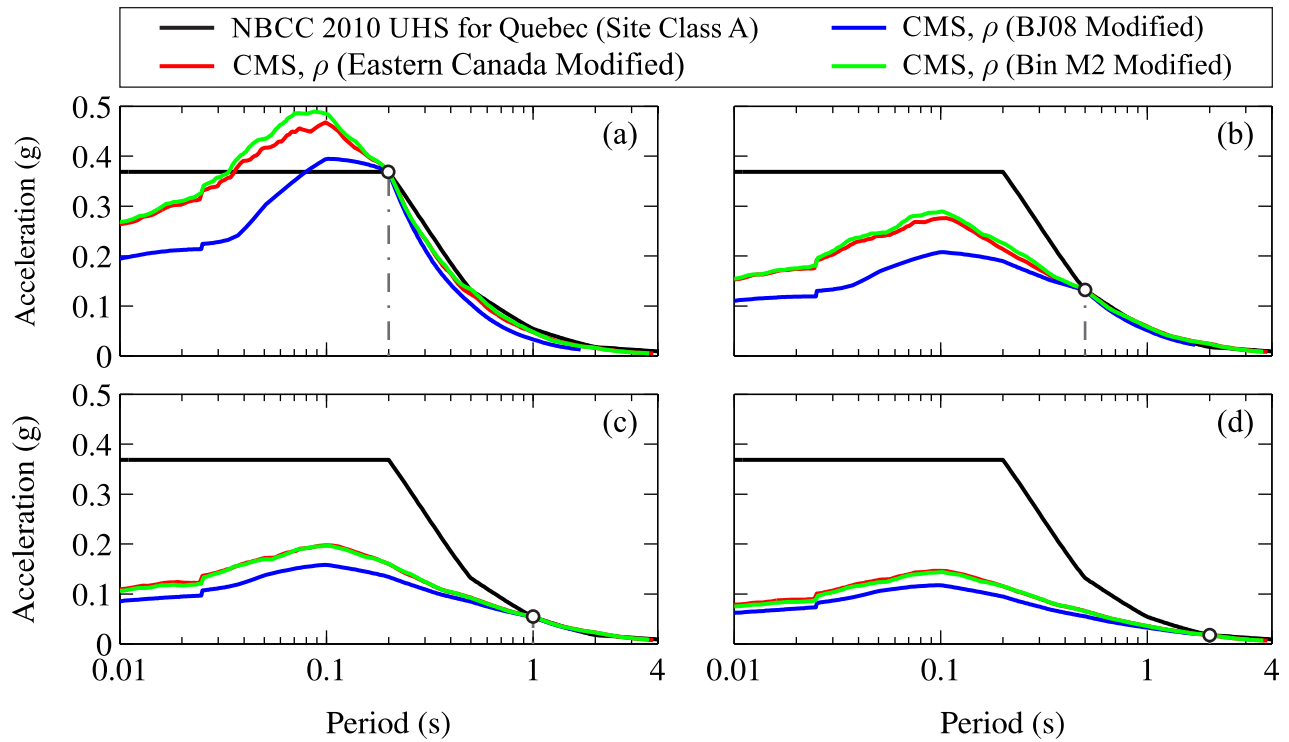


Figure 18. CMS computed using magnitude-based ρ s for Eastern Canada and by matching to NBCC 2010 prescribed UHS for Quebec at: (a) $T^* = 0.2$ s, (b) $T^* = 0.5$ s, (c) $T^* = 1$ s, and (d) $T^* = 2$ s.

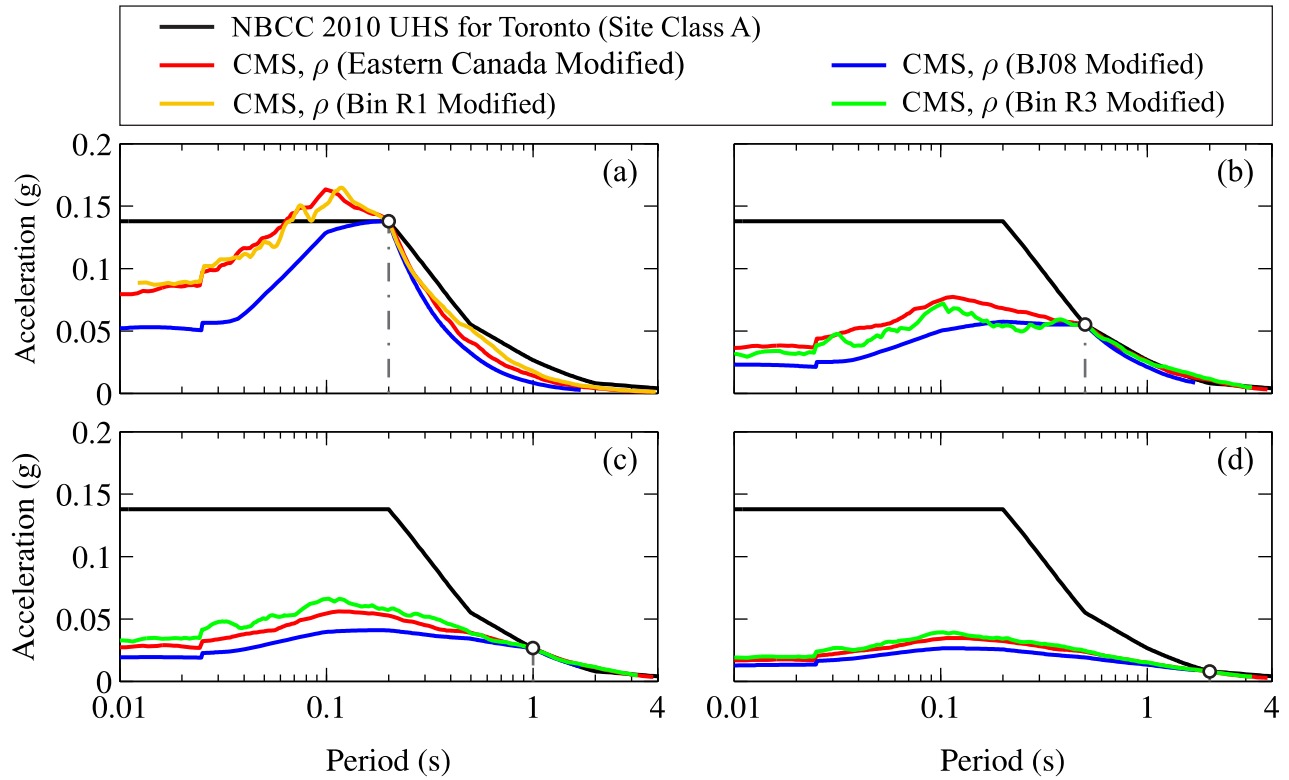


Figure 19. CMS computed using distance-based ρ_s for Eastern Canada and by matching to NBCC 2010 prescribed UHS for Toronto at: (a) $T^* = 0.2$ s, (b) $T^* = 0.5$ s, (c) $T^* = 1$ s, and (d) $T^* = 2$ s.

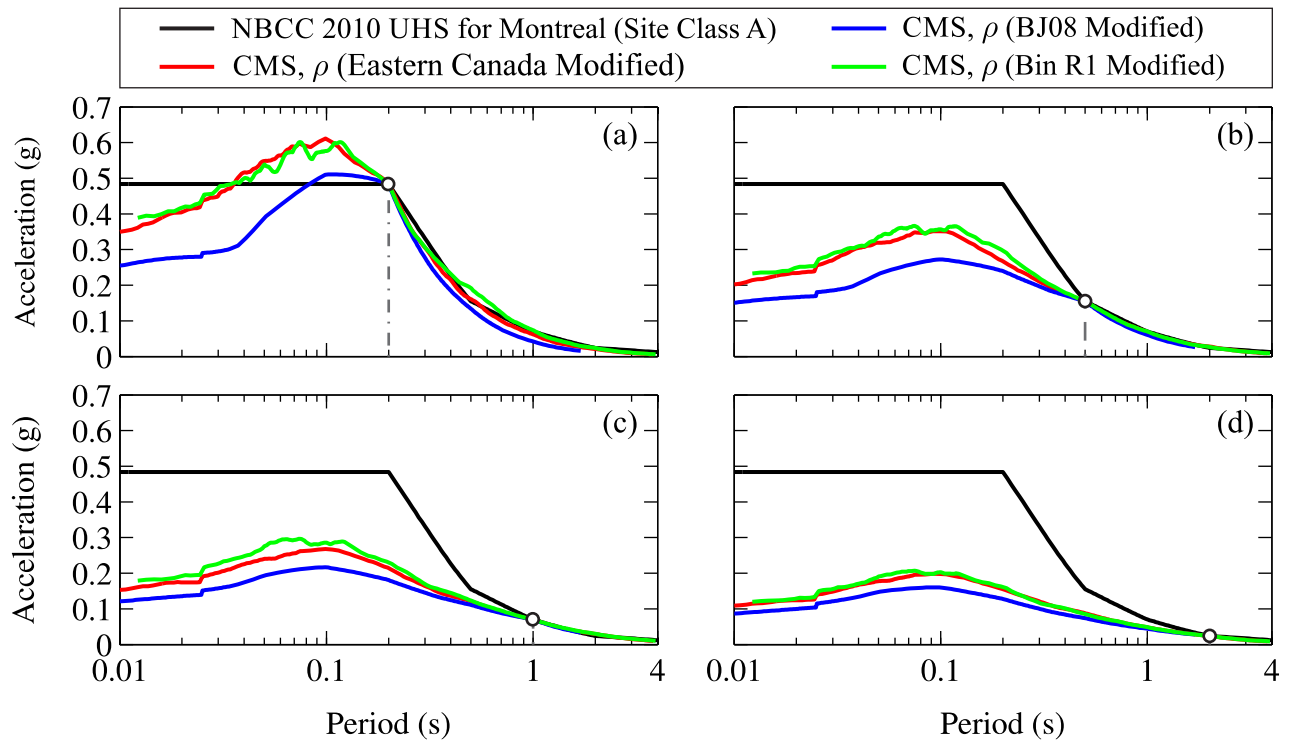


Figure 20. CMS computed using distance-based ρ s for Eastern Canada and by matching to NBCC 2010 prescribed UHS for Montreal at: (a) $T^* = 0.2$ s, (b) $T^* = 0.5$ s, (c) $T^* = 1$ s, and (d) $T^* = 2$ s.

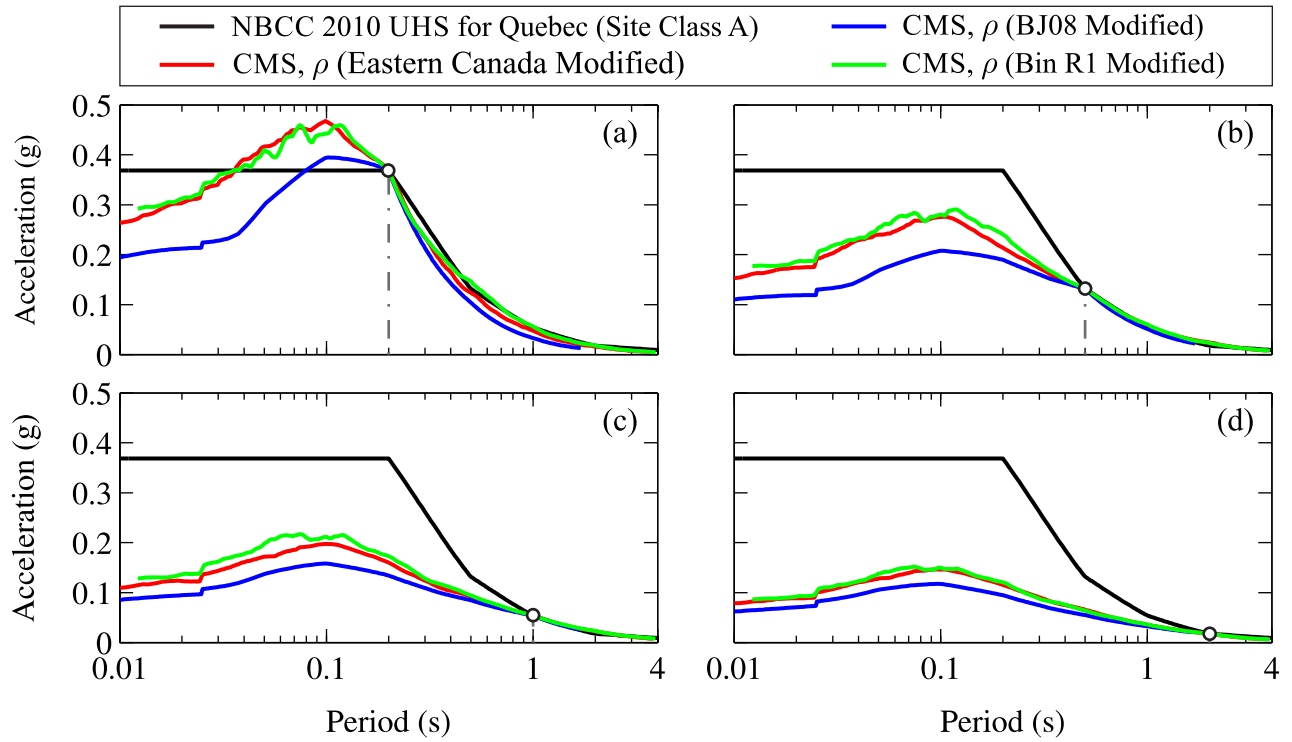


Figure 21. CMS computed using distance-based ρ s for Eastern Canada and by matching to NBCC 2010 prescribed UHS for Quebec at: (a) $T^* = 0.2$ s, (b) $T^* = 0.5$ s, (c) $T^* = 1$ s, and (d) $T^* = 2$ s.